ANALYTICAL MODELLING AND NUMERICAL SIMULATION OF PLASMA – ASSISTED 2D GRAPHENE SOLAR CELLS

A Project Report
Submitted in the Fulfillment of the Requirements
For the Degree of

MASTER OF SCIENCE

in

Physics

by

Shreya Vasu

Roll No. 2K22/MSCPHY/51

Shikha Singh

Roll No. 2K22/MSCPHY/35

Under the supervision of

Prof. Suresh C. Sharma

Department of Applied Physics

DELHI TECHNOLOGICAL UNIVERSITY
(Formerly Delhi College of Engineering)
Shahbad Daulatpur, Main Bawana Road, Delhi – 110042, India

June, 2024

DEPARTMENT OF APPLIED PHYSICS
DELHI TECHNOLOGICAL UNIVERSITY
(Formerly Delhi College of Engineering)
Shahbad Daulatpur, Main Bawana Road, Delhi – 110042, India

CANDIDATE'S DECLARATION

We, **SHREYA VASU** and **SHIKHA SINGH**, students of **M.Sc. Physics** hereby declares that the project report titled "***Analytical Modelling and Numerical Simulation of Plasma – Assisted Graphene Solar Cells***" which is submitted by us, under the supervision of **Prof. SURESH C. SHARMA**, to the Department of Applied Physics, Delhi Technological University, Delhi in the fulfilment of the requirement for the award of the degree of Master of Science in Physics is an authentic record of our own work, carried out during the period from July 2023 to June 2024. The matter presented in this report has not been copied from any source without proper citation. This work has not previously formed the basis for the award of any Degree, Diploma Associateship, Fellowship or other similar title or recognition.

The work has been accepted in a peer reviewed Scopus indexed conference with the following details:

Title of the Paper: Analytical Modelling and Numerical Simulation of Plasma-Assisted Graphene Solar Cells

Author names: Shreya Vasu, Shikha Singh, Suresh C. Sharma

Name of Conference: Recent Advances in Functional Materials (RAFM-2024), Atma Ram Sanatan Dharma College, Delhi University

Conference Date: 16.03.2024

Have you registered for the conference (Yes/No)?: Yes

Date of paper communication: 18.04.2024

Date of acceptance: 06.06.2025

Shreya Vasu (2K22/MSCPHY/51)

Shikha Singh (2K22/MSCPHY/35)

DEPARTMENT OF APPLIED PHYSICS

DELHI TECHNOLOGICAL UNIVERSITY

(Formerly Delhi College of Engineering)

Shahbad Daulatpur, Main Bawana Road, Delhi – 110042, India

CERTIFICATE

I hereby certify that the Project Report titled "***Analytical Modelling and Numerical Simulation of Plasma – Assisted Graphene Solar Cells*** " which is submitted by **SHREYA VASU** and **SHIKHA SINGH**, to the Department of Applied Physics, Delhi Technological University, Delhi in the fulfilment of the requirement for the award of the degree of Master of Science, is a record of the project work carried out by the student under my supervision. To the best of my knowledge this work has not been submitted in part or full for any Degree or Diploma to this University or elsewhere. I, further certify that the publication and indexing information by the students is correct.

Place: Delhi **Prof. Suresh C. Sharma**

Date: 07/06/2024

DEPARTMENT OF APPLIED PHYSICS

DELHI TECHNOLOGICAL UNIVERSITY

(Formerly Delhi College of Engineering)

Shahbad Daulatpur, Main Bawana Road, Delhi – 110042, India

ACKNOWLEDGEMENT

We wish to express our sincere gratitude to our supervisor **Prof. Suresh C. Sharma** for the guidance and mentorship he has provided for this project. He was instrumental in helping us understand the tasks and achieve the results. He was ready to always clear our doubts regarding any obstacles we faced in the project. Without his constant support and motivation, this project would not have been successful.

Place: Delhi SHREYA VASU

Date: 07/06/2024 SHIKHA SINGH

Table of Contents

ABSTRACT

Graphene, largely because of its dynamic properties such as enhanced carrier mobility, has emerged as an important photovoltaic material for increased photo energy conversion. The efficiency of a perovskite photovoltaic cell can be improved by replacing the “hole transport layer” (HTL) with a layer of graphene. This study demonstrates how growing graphene using the PECVD technique affects the device efficiency. An ITO/PCBM/$CsPbI_3$/Graphene model is simulated using the software SCAPS-1D where $CsPbI_3$ is used as absorber, PCBM as the ETL and Graphene as the HTL. A numerical relation between solar cell efficiency and the plasma parameters is established and the numerically calculated efficiency is compared with that of the simulated model. It is also found that, upon introducing an increment in electron and ion density of graphene sheet, the efficiency of device reduces due to an inverse relation with the debye length, whereas, introducing an increment in the electron and ion temperatures results in the enhancement of the device efficiency due to a linear relation with the debye length, thereby showing that altering the different plasma parameters at an optimum thickness of the absorber layer and HTL, the device efficiency can be raised, which would better its performance and real-world application.

List of Figures

Chapter 1: Introduction

Chapter 2: Model

Chapter 3: Results & discussion

List of Tables

List of Symbols and Abbreviations

Parameters	Symbols
Efficiency of solar cell	H
Power Input	P_{in}
Thickness of Graphene layer	t
Fill Factor	FF
Short Circuit Current Density	J_{SC}
Open Circuit Voltage	V_{OC}
1D donor concentration	N_{1D}
Boltzmann Constant	K_B
Oxide Permittivity	ε_{ox}
Debye Length	λ_D
Electron Debye Length	λ_e
Ion Debye Length	λ_i
Electron Temperature	T_e
Ion Temperature	T_i
Electron Density	n_e
Ion Density	n_i
Conduction Band	CB
Valence Band	VB
Donor Concentration	N_D
Acceptor Concentration	N_A
Quantum Efficiency	QE_{eff}
Band Gap	E_g
Dielectric Permittivity	ϵ_r
Electron Affinity	χ
Indium Tin Oxide	ITO
Phenyl-C61-butyric acid methyl ester	PCBM
Metal work function	Φ
Graphene based perovskite solar cell	GrPrSC
Generation rate of Electrons	G_n
Generation rate of Holes	G_p
Electronic charge	q
Hole current density	J_p
Electron current density	J_n
Power Conversion Efficiency	PCE_{eff}
Air Mass spectrum	AM
Reverse saturation current	J_o

CHAPTER 1

INTRODUCTION

1.1. Introduction to Solar Cell

Any device that directly converts light energy into electrical energy is called a solar cell, also referred to as a photovoltaic cell. Another term for this phenomena is the photovoltaic effect. Several types of solar cells have been developed and researched in an effort to reach high efficiency since the discovery of the photovoltaic effect. The type of solar cell and building materials used in a photovoltaic device impact how well it works overall[7]. These days, the majority of solar cells that are commonly utilized in commercial applications have an efficiency of up to 15% and are based on silicon. Unlike batteries or fuel cells, solar cells don't require fuel or chemical processes to operate. They generate power by utilizing the photovoltaic effect.

1.1.1 Construction

A solar cell is typically made of an n-type layer of crystalline silicon. The uppermost layer is referred to as the "**Emitter layer**". The "**base**," or second layer, is composed of a p-type semiconductor. They create a p-n junction when combined. The surface is coated with an anti-reflective material to stop incident light energy from being wasted through reflection. A solar photovoltaic panel is an arrangement of several solar cells grouped together and orientated in a single plane. Solar cells are generally connected in series to give voltage, but connecting them in parallel produces a bigger current.

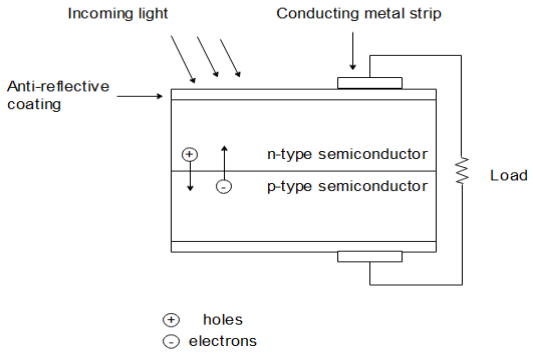

Fig 1.1 Structure of a solar cell

1.1.2 Working

In a photovoltaic cell, the semiconductor material has the ability to either absorb or reflect back photons that strike it. When a certain quantity of photons is absorbed, the electrons in the semiconductor material's atom become free electrons. The same is true with holes.

As a result, the junction thermal equilibrium is disturbed and a depletion layer is formed. The potential barrier prevents electrons and holes from moving beyond it, and the buildup of charges across the junction produces a voltage known as the photovoltaic emf.

1.1.3 Efficiency

The ratio of energy output to input energy obtained in a solar cell is known as the cell's efficiency. It is given by the following expression

$$\eta = \frac{P_{max}}{P_{inc}} \tag{1.1}$$

$$P_{max} = FF \times V_{OC} \times I_{SC} \tag{1.2}$$

where,
P_{inc} stands for Incident photon power and P_{max} for maximum power. The fill factor is represented by FF, the open circuit voltage by V_{OC}, and the short circuit current by I_{SC}. [7]
Fill factor can be given by the following expression,

$$FF = \frac{V_{max} \times I_{max}}{V_{OC} \times I_{SC}} \tag{1.3}$$

here,
V_{max} is the maximum voltage
I_{max} is the maximum current [7]

1.1.4 Layers in Solar Cell

The five primary layers of a solar cell are “glass”, the “absorber”, the “back metal”, the “hole transport layer”, and the “electron transport layer”.

(a) *Glass* - The translucent rear layer of glass-glass solar panels lets light enter the module from the front and isn't absorbed by the solar cells. Since the amount of light that reaches the solar cells is the single factor that determines power output, this increases cell to module losses and reduces the power generated.

(b) *Electron Transport Layer (ETL)* – In solar cells, electrons are injected from the absorber layer into the “electron transport layer” (ETL), where they are subsequently carried by the “electron transporting materials” (ETM) and collected by the electrode.

(c) *Hole Transport Layer (HTL)* – The extraction and transport of holes, surface passivation, perovskite crystallization, device stability, and cost are all significantly influenced by hole-transporting layers (HTLs), which are a crucial part of inverted, p–i–n PSCs.

(d) *Absorber* – Electrons in the absorber layer of a solar cell are excited by light to migrate from their lower-energy “ground state,” where they are bonded to certain atoms in the solid, to a higher “excited state,” where they can move freely inside the solid.

(e) *Black Metal* – When ordinary silicon's surface is scratched to create microscopic, nanoscale pits, black silicon is created. These pores cause the silicon to turn black instead of gray, and more importantly, they trap more light—a necessary component of solar cells that work well.

By altering the composition of the various layers, a solar cell's efficiency can be increased.

1.2 Graphene Based Solar Cells

Graphene is a two-dimensional substance composed of carbon atoms arranged in a hexagonal configuration. Though it is up to five times lighter than aluminum, it has the same density as carbon fiber and is structurally similar to graphite. Its strength can outperform steel by up to 200 times, even though it is much thinner. Graphene is transparent, flexible, and waterproof, but it also has outstanding thermal and electrical conductivity, which must be considered.

The use of graphene for renewable energy has been a primary scientific goal since its discovery, and renewable energy is a popular topic in the twenty-first century. One of the industries with the quickest growth is solar photovoltaics, which currently generates more than 2% of global electricity. The most common type of photovoltaics is silicon-based, but they are not very cost-effective. Different options were therefore devised. Since their invention in 2009, perovskite solar cells, or PSCs, have already achieved a 25% efficiency. PSCs are less expensive than those made of silicon. Interface engineering's ability to integrate graphene and similar two-dimensional materials boosts efficiency, which is a promising development for PSCs and the photovoltaics industry overall.

1.2.1 Structure of graphene

Three nearby carbon atoms combine to form graphene through sp^2 hybridization. Together, they form a monolayer graphene sheet with a planar shape that is referred to as a honeycomb network. The structure of graphene can be two or three dimensions.

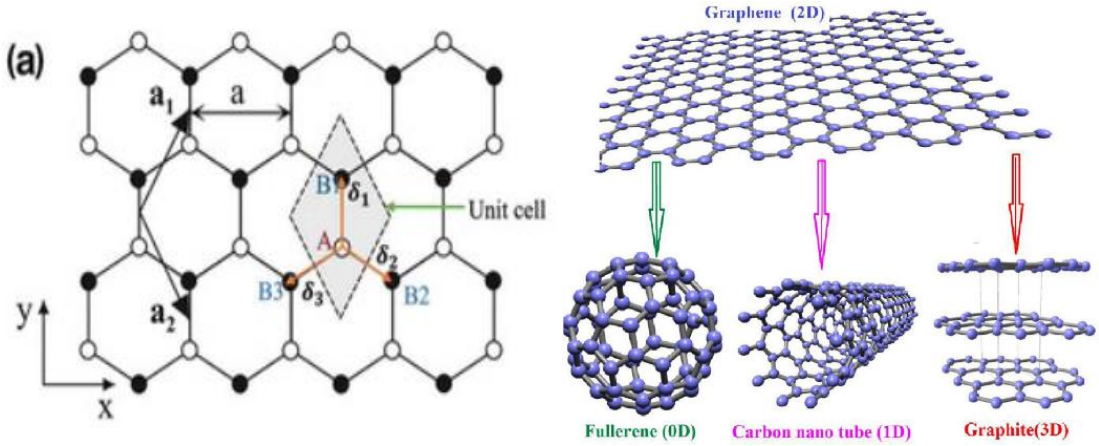

Fig 1.2 (a) Monolayer graphene honeycomb lattice; white and black circles, respectively, represent the carbon atoms at sites A and B, (b) different carbon allotropes of various dimensions are formed from graphene [9].

1.2.2 Growth of graphene layer using plasma

The production of graphene sheets involves two fundamental techniques: a top-down and bottom-up approach. The flowchart for the various techniques is shown below.

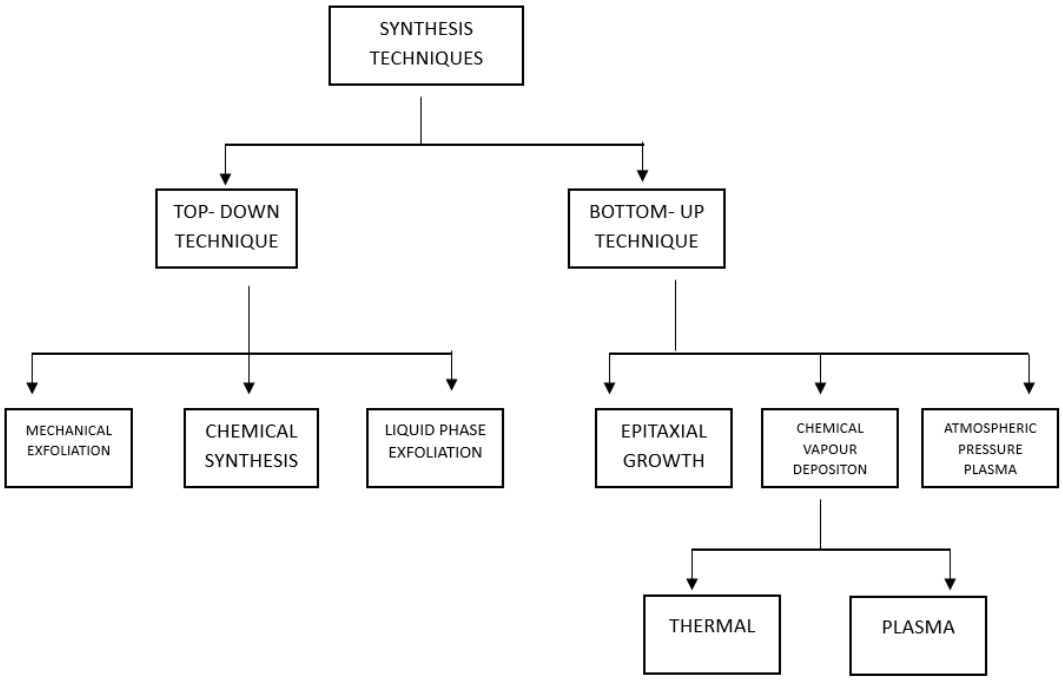

Fig 1.3 Various synthetic methods for producing graphene sheets [8].

We are mainly focusing our study on fabrication of graphene sheet using plasma technique. This technique is called **Plasma- enhanced chemical vapor deposition (PECVD)**

The three steps of the PECVD process for graphene synthesis are precursor delivery, breakdown, and graphene generation.

1. *Introduction of Precursor*: A gaseous precursor is present in the plasma zone, where it can break down into more manageable reactive reagents like CO and H_2.
2. *Creation of Plasma*: A high frequency electric field or alternative methods are used to form a plasma.
3. *Chemical Reaction*: In the plasma, the precursor gas experiences chemical reactions that result in the production of reactive species.
4. *Thin Film Deposition*: On the substrate, carbon takes the form of graphene as the residual gases leave the plasma zone. The entire process is completed in a matter of seconds.
5. Subsequently, the chamber is cooled, and the substrates that have been deposited with graphene are removed. They are preserved for additional examination.

An overview of the method is shown in figure below [8].

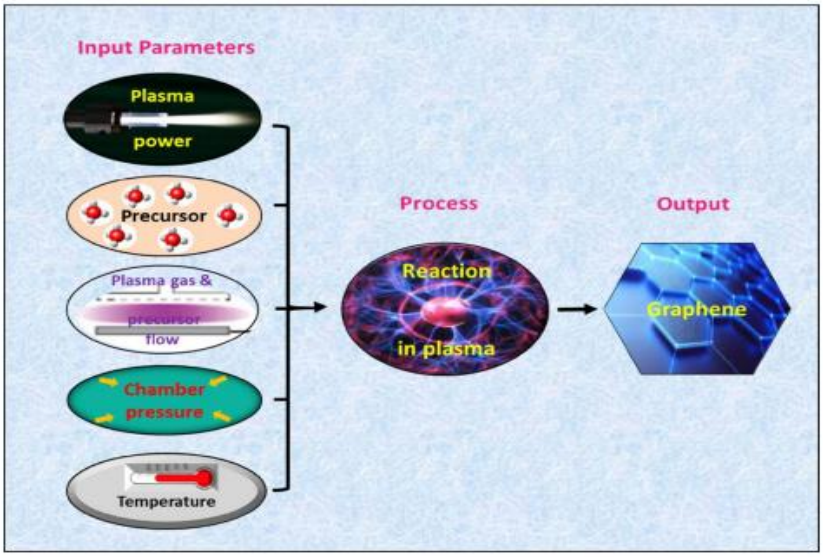

Fig 1.4 An overview of PECVD [8].

1.2.2.1 Input parameters

The following are examples of input parameters: temperature, chamber pressure, precursor, and plasma power. The conventional industrial microwave (MW) and radio frequency (RF) frequencies for the synthesis of graphene are 2.45 GHz and 13.56 MHz, respectively.

Precursor: It goes by the names monomer and feedstock as well. The pace at which precursor flows determines the synthesis of graphene. There must be carbon compounds in the precursor. Gaseous hydrogen (H_2) is usually used with a precursor in the production of graphene. The ratio of gas to precursor plays a significant role in the synthesis process.

Chamber pressure: While high vacuum pressure is needed to achieve a high production rate in microwave plasma, sub-atmospheric pressure has a poor production rate.

Temperature: Precursors vary in temperature according to the C-H bonding energy. Lower temperature PECVD is made feasible by the active and energetic ions and electrons that can help break down molecular chains.

1.2.2.2. Growth mechanism of graphene

Using the RF-PECVD technique, vertical graphene grows in three stages, i.e,

(i) initial carbon film nucleation and island development
(ii) initial graphene sheet growth and
(iii) subsequent growth and net-like graphene sheet synthesis. Ref. [9]

1.2.3 Application of graphene based solar cells

Three layers of graphene can be used in a solar cell: the carrier transport layer, the photoactive layer, and the electrodes.

1. **As transparent conducting anode:** Graphene is one of the best materials to be used as transparent conducting electrode/anode due to its exceptional transparency and low sheet resistance. By replacing the commonly used materials, indium tin oxide (ITO) and fluorinated tin oxide (FTO), it can reduce prices while enhancing flexibility and stability.
2. **As transparent conducting cathode:** It is the perfect material to utilize as a transparent conducting cathode because of its high conductivity, extremely high mobility, and transparency.
3. **As catalytic counter electrode:** The photovoltaic performance is enhanced by graphene's flexibility, high catalytic activity, low charge transfer resistance, and ease of production at ambient temperature.
4. **As active layer:** Graphene has the potential to be used as a light harvesting material because of its heterostructure and light harvesting capabilities.
5. **As carrier transport layer:** Graphene can be employed as a carrier carrying layer because of its great carrier mobility. Moreover, its carrier mobility is high.
6. **As Schottky junction:** The performance of solar systems was improved by graphene-based materials that showed exceptional mobility and conductivity and improved the mechanism of electron transport.
7. **As electron transport layer:** High mobility and conductivity makes graphene suitable as electron transport layer.
8. **As hole transport layer:** Increased hole extraction and electron blockage while improving the performance of the solar cell makes graphene an exciting candidate for hole transport layer.

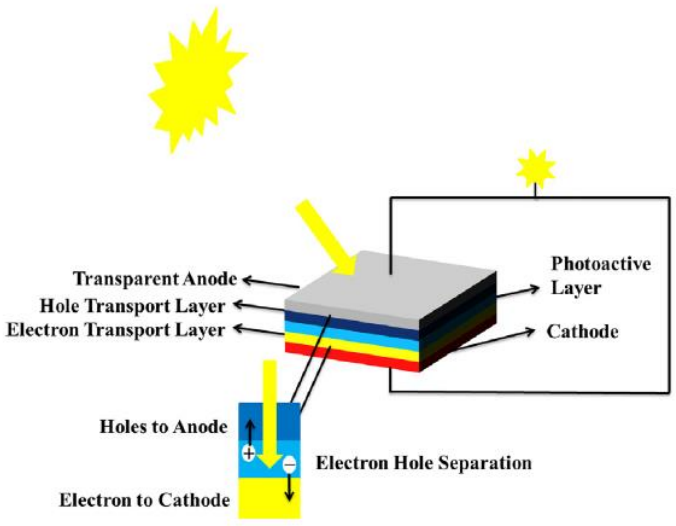

Fig 1.5 In a solar cell, a photoactive layer is positioned in between the electron and hole transport layers and the back and front electrodes. [7]

1.2.4 Advantages and Disadvantages of graphene based solar cells

1.2.4.1 Advantages

1. Because graphene sheets are extremely thin, making graphene solar cells is inexpensive because it only needs a little amount of raw materials.
2. Because graphene is transparent and flexible, it is used in aircraft and spacecraft.
3. Solar cells require conductive materials that allow light to flow through them. The enhanced conductivity and transparency of graphene are useful in this situation. Graphene is a great conductor, but it is not particularly good at absorbing the current that is produced inside the solar cell.
4. Graphene has a larger spectrum of capture and absorbs 2.3% of radiation. (2010) Bonaccorso and co workers.
5. The exceptional mobility of graphene carriers (μ=20,000 cm^2/Vs) combined with its low sheet resistance make it a prospective substitute for Indium doped Tin Oxide (ITO) as a photo anode. Chen and colleagues (2008); Rowell and McGehee (2011).
6. Charge collection and release are brought about by the huge surface to mass ratio (2630m2/g), which improves performance. Pigney and associates, 2001. [7]
7. The superior chemical activity of graphene makes it ideal for application as a photoactive layer in solar cells. Yan et al. (2010); Liu et al. (2008); Gupta et al. (2011).
8. The counter electrode's catalytic activity is altered and the charge transfer process is enhanced by a larger chemically active surface area. High current density, improved charge transfer activity, and low sheet resistance were all demonstrated by chemically functionalized graphene. (Mayhew-Roy and others, 2010).
9. Moreover, by accelerating the carrier separation and diffusion process, graphene/semiconductor Schottky connections enhance performance. [7]

Given its ability to promote efficient energy absorption, graphene might be the material of choice for solar cell production.

1.2.4.2 Disadvantages

1. Graphene is difficult to deal with in solar cells, which results in low production and the possibility of hydrophobicity.
2. Graphene oxide has limited control over post-preparation functionalization and low electrical and thermal conductivity when employed in solar cells.
3. The application of reduced graphene oxide (rGO) results in hydrophobicity. It is challenging to deal with and has characteristics specific to the production process.

Graphene is still regarded as the best material out of all those that are accessible, despite this issue.

1.3 SCAPS Software

A variety of factors and physical characteristics are taken into consideration when simulating solar cell operation using SCAPS (Solar Cell Capacitance Software). It makes it possible for engineers and scientists to model and evaluate the electrical behavior of solar cells under varied conditions. Usually, it only works with one dimension.

It is crucial to be able to use the program to simulate the capacitance-voltage (C-V) characteristics of solar cells in order to understand their electrical properties. It can provide insight into how different building practices, materials, and architectural styles impact solar cell efficiency.
Some photovoltaic parameters include J_{SC}, V_{OC}, FF and PCE_{ff} etc.

1.3.1 User interface

Fig 5: SCAPS template

Software references have been included below [20-27].

CHAPTER 2

MODEL

TOPIC: Analytical modelling and numerical simulation of plasma - assisted graphene solar cells

2.1 Literature Review

At the initial stage of my research, I read the following papers under the guidance of my supervisor:

2.1.1 Effect of thickness on the efficiency [4].

In order to create industrial-grade solar cells, the authors of this work employed the PECVD (Plasma Enhanced Chemical Vapour Deposition) technique to manufacture graphene in continuous layers directly on planar n-type silicon. The work function, V_{OC}, and PCE may all be greatly increased by adjusting the graphene thickness. The authors' suggested schematic diagrams are displayed below [4].

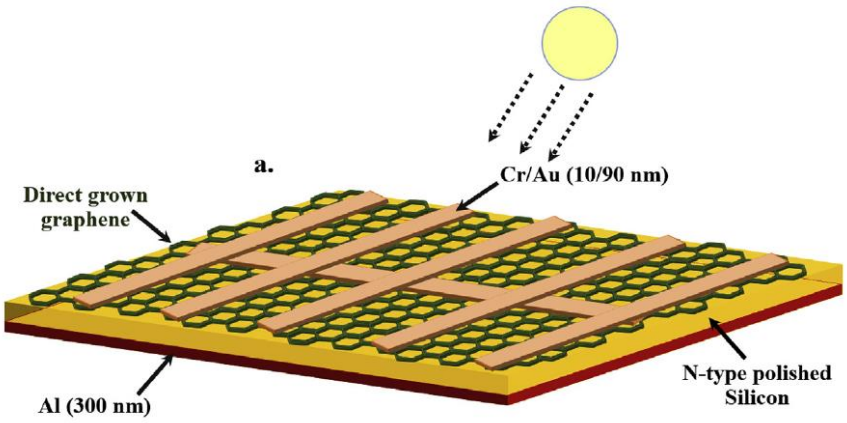

Fig 2.1 (a) Diagram of the device used to demonstrate graphene-silicon grown directly Schottky junction solar cells [4].

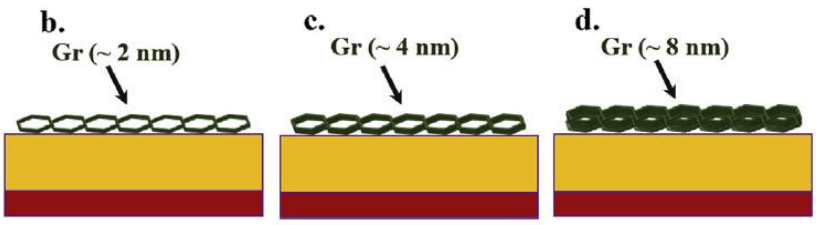

Fig 2.2 (b-d): Diagrams representing the growth times of 2, 4, and 8 nm thin graphenes at 2.5, 3.5, and 4.5 hours, respectively [4].

This technique used multi-layer graphene that was directly synthesized on silicon. The best results were obtained by varying the graphene's thickness and including an additional polymer layer. With its balanced conductivity and transparency, the 4 nm thick graphene device performed at its best. Using a direct growth technique, the author's efficiency in bare silicon was 5:51%; this was further increased to 9:18% following PMMA coating and doping [4].

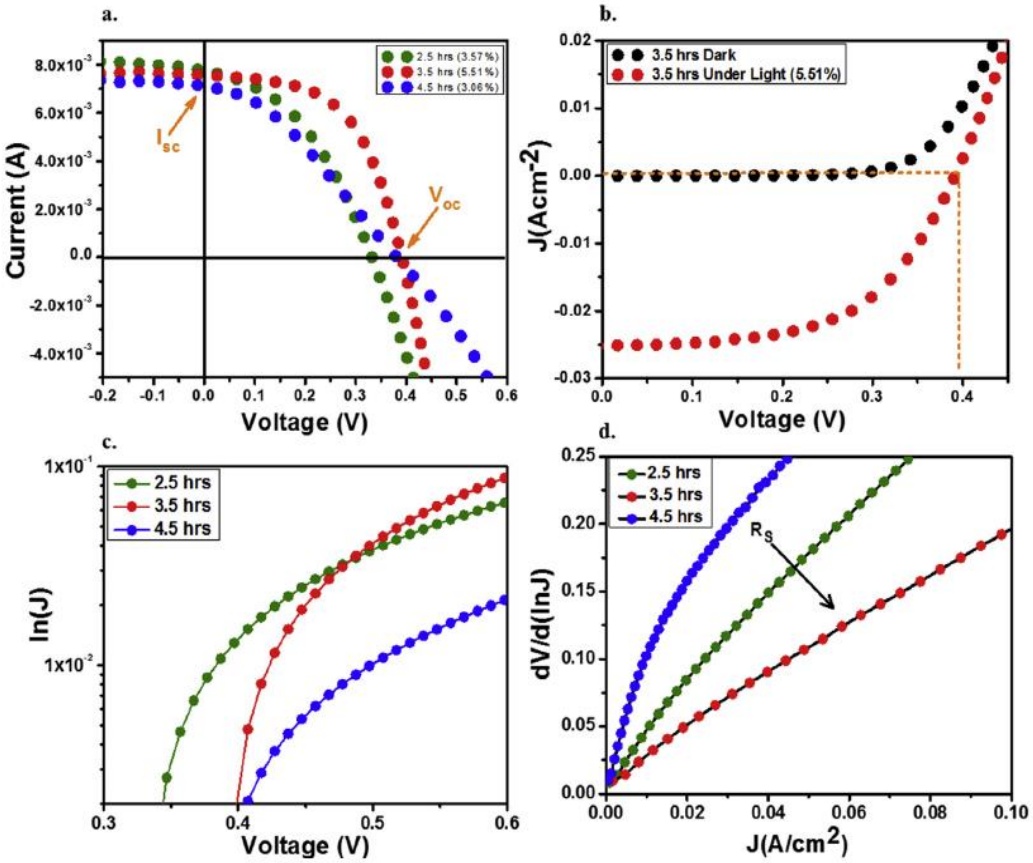

Fig 2.3 Comparing direct-grown graphene on bare silicon with varying growth durations or thicknesses in terms of its photovoltaic characteristics and performance parameters.

(a) Current vs Voltage curves under light with thickness variation.
(b) J-V curves in both dark and light conditions, with an optimal thickness of 4 nm.
(c) By computing the ideality factor, a J-V plot on a semi-log scale can be used to verify a diode's ideal behavior.
(d) Plot of relationship between current density and dV/d(ln J), which yields series resistance. Depending on the thickness, the arrow direction represents a reduction in series resistance [4].

2.1.2 Analysis of weak charge screening in 2D Semiconductors [3].

In this paper, in order to properly characterize the electrostatic behavior in thin semiconductors, the authors have demonstrated that the 3D electrostatic models do not correctly describe semiconductors thinner than the 3D Debye length [3]. As a result, they have concluded that new 2D specialized electrostatic models are required [3].

They have taken a simple perturbation in 2D semiconducting material and have solved for Poisson's equation. They have then determined the 2D Debye screening length, the analytical expressions for the electrostatic potential, its Fourier representation etc.

From the paper,

$$\lambda_D = \frac{kT}{q}\frac{2\varepsilon_{ox}}{q_{N_{2D}}}, \tag{2.1}$$

where λ_D = 2D Debye screening length.
Then solve the Poisson equation with appropriate boundary conditions to get the expression for potential.
The general solution is:

$$V(x,y) = \frac{qN1D}{4\epsilon_{ox}}\sum_{n=1}^{\infty}\frac{2sin(\lambda_n h)}{\lambda_n(h+cos^2(\lambda_n h)\lambda_D)}\, sin(\lambda_n y)\, e^{-\lambda_n x} \tag{2.2}$$

And for y = h

$$V_{2D}(x) = V(x,y=h) = \frac{qN1D}{2\epsilon_{ox}}\sum_{n=1}^{\infty}\frac{(\lambda_n {\lambda_D}^2/h)e^{-\lambda_n x}}{{\lambda_n}^2{\lambda_D}^2+1+\lambda_D/h} \tag{2.3}$$

2.1.3 Review paper: Recent progress in Graphene incorporated Solar Cell Devices.

In this review paper, the PCE of several graphene solar cell devices has been studied by the writers. They have looked into a variety of solar cell systems, including hybrid, inorganic, and organic designs. The paper describes the various layers of the solar cell and the role they play in the photovoltaic generation of electricity in solar cells.

They have noted the following observations:

1. The efficiency for DSSCs with graphene counter electrode was 4.5%, which is similar to the 6.3% efficiency of a device based on Pt counter electrode.
2. The efficiency of the Gr/Silicon nanowire based Schottky device was 10.30%, whereas the Gr/Silicon nanohole based Schottky device was 8.71%.
3. The performance of bulk hetero-junction solar cell devices has risen from 5.9% to 7.5% with the use of GO as the electron transport layer [7].

2.1.4. Effects of process parameters on vertically grown graphene sheets using PECVD method [6].

In order to investigate the process factors and their impact on vertically oriented graphene sheets (VOGS) produced in a PECVD system using a reactive gas mixture of Ar + H_2 + C_2H_2, the authors of this work have developed a numerical model. The input plasma power and total gas pressure are two examples of these parameters [6].
They have noticed the following things:

1. From the bulk plasma area to the substrate surface, there is a discernible drop in the concentrations of various plasma species.
2. The plasma zone exhibits a measurable loss of energetic electrons for both low input power (for constant gas pressure) and high pressure (for constant input power).
3. When input plasma power is increased from 100 to 300 W, the growth rate of VOGS increases. However we start noticing a drop in the growth rate of VOGs when the plasma power is increased even more than this value [6].

After reading these articles, it struck me to learn more about the efficiency and operation of solar cells as well as the several plasma-based growth methods used to expand the graphene layer on the device. I was able to create a link between the thickness of the graphene layer and the plasma parameters using the Debye length thanks to the papers in [3] and [4].

2.2 Simulated device structure

We simulate a model of ITO/PCBM/$CsPbI_3$/Graphene (GrPeSC) using the SCAPS 1D program. Initially, a 0.050 μm-thick layer of ITO serves as the top electrode. We designate PCBM as the ETL, measuring 0.010 μm thick, and an HTL of plasma aided graphene, measuring 0.068 μm thick, to collect electrons and holes from the absorber layer. A 0.5 μm-thick layer of $CsPbI_3$ is taken into account as the absorber in the PeSC design. In our experiment, we vary the thickness of the absorber layer from 0.1 μm to 1 μm and the graphene layer from 0.001 μm to 0.01 μm. The results are presented in the results and comments. We also include Au as the cathode, which has a work function of 5.3 eV. During the simulation, the air mass spectrum of AM 1.5 radiation was assumed, keeping a working temperature of 300K, frequency of 10^6 Hz and the device was operated under illuminated (ON) condition.

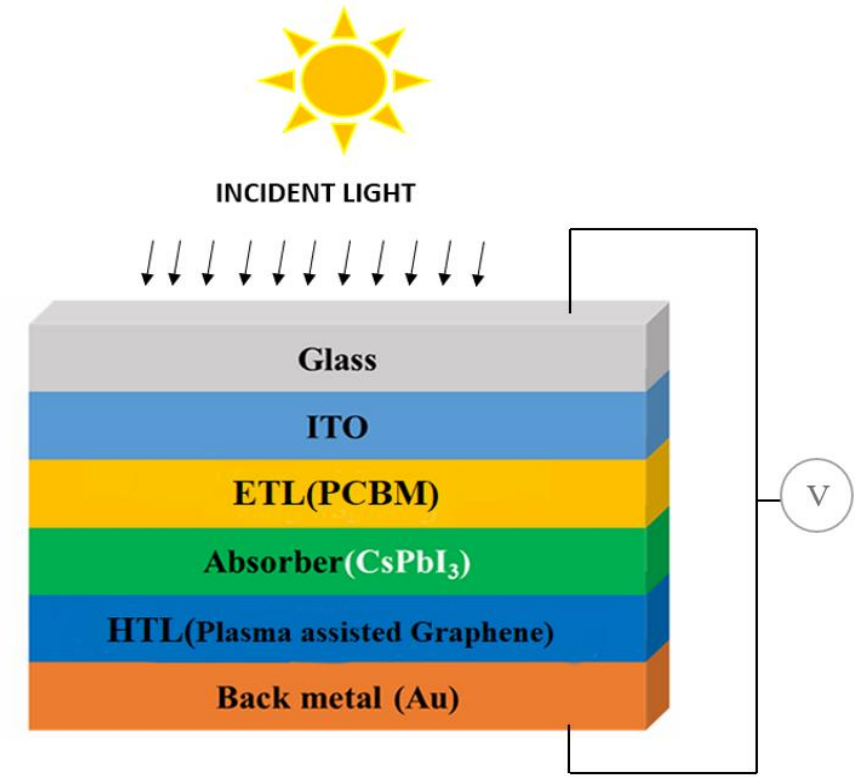

Fig. 2.4 Schematic diagram of ITO/PCBM/$CsPbI_3$/Graphene solar cell

Marc Burgelman created the one-dimensional numerical modeling and simulation program called SCAPS 1D. [20], [21], [22], [23], [24], [25], [26], [27]. There are certain one dimensional equations governing the charge carriers and conduction of semiconductor under the steady state. By resolving those equations, this software facilitates understanding of the basic characteristics of solar cells and pinpoints the key elements influencing their operation.

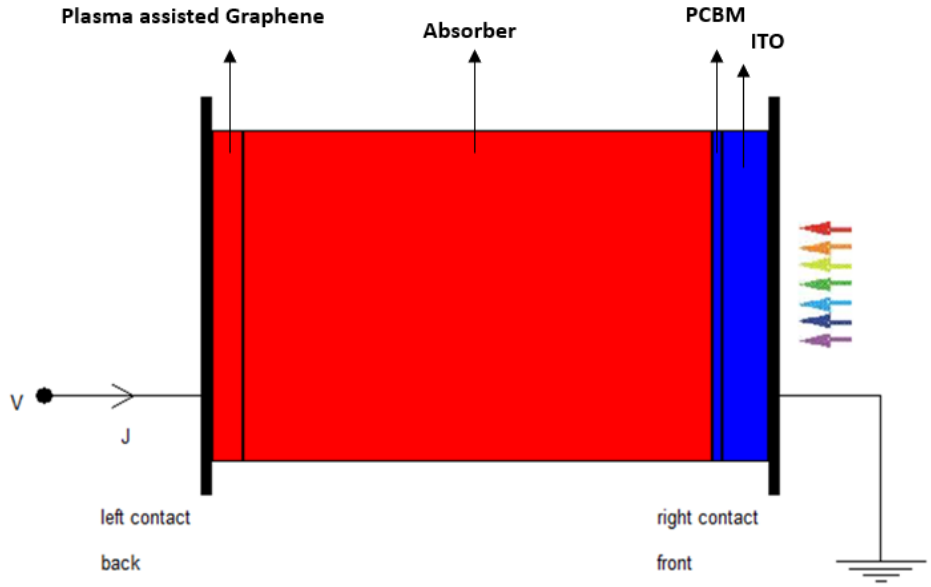

Fig. 2.5 Simulated structure of the GrPrSC model using SCAPS-1D software.

We know the Poisson's equation to be,

$$\nabla(\varepsilon.\nabla\psi) = -\rho \tag{1}$$

The equation of continuity for negative charged carriers is given as,

$$\frac{\partial n}{\partial t} = \frac{1}{q}\nabla(J_n) + G_n - R_n \tag{2}$$

The equation of continuity for positive charged carriers is given as,

$$\frac{\partial p}{\partial t} = \frac{1}{q}\nabla(J_p) + G_p - R_p \tag{3}$$

The air mass spectrum of AM 1.5 of the radiation was assumed during the simulation, keeping a working temperature of 300K, frequency of 10^6 Hz and the device was operated under illuminated (ON) condition.

Table 2.1 Simulation parameters of ITO, Absorber, ETL and HTL.

S.N.	Parameter	ITO	Absorber	ETL	HTL
1	Thickness (nm)	500	Variable	10	33.4
2	Band Gap (eV)	3.5	1.694	2.0	0.098
3	Electron affinity (eV)	4	3.95	3.9	4.8
4	Layer Relative permittivity	9	9	3.9	10
5	CB effective density of states ($1/cm^3$)	2.2×10^{18}	1.1×10^{20}	2.5×10^{21}	3×10^{9}
6	VB effective density of states ($1/cm^3$)	1.8×10^{19}	8.2×10^{20}	2.5×10^{21}	3×10^{9}
7	Electron mobility ($cm^2/V.s$)	20	25	0.2	10×10^{5}
8	Hole mobility ($cm^2/V.s$)	10	25	0.2	10
9	Shallow uniform acceptor density ($1/cm^3$)	-	1×10^{15}	-	2.328
10	Shallow uniform donor density ($1/cm^3$)	1×10^{21}	-	2.93×10^{17}	1×10^{19}
11	References	[29],[41], [42],[43]	[2],[44]	[2],[42],[43], [45],[46],[47]	[37],[38]

Table 2.2 Parameters used for metal contacts

S.N.	Parameter	Right contact (front)	Left contact (back)
1	Electron surface recombination velocity ($cm.s^{-1}$)	1×10^7	1×10^5
2	Work function of metal used (Au) (eV)	3.8415	5.3
3	Hole surface recombination velocity ($cm.s^{-1}$)	1×10^5	1×10^7

Table 2.3 Parameters used for defect in solar cells

S.N.	Parameter	Graphene/$CsPbI_3$
1	Type of defect	68.3
2	Capture cross section of electrons (cm^2)	0.098
3	Capture cross section of holes (cm^2)	4.8
4	Energy distribution	10
5	Reference for def. energy level (eV)	3×10^9
6	Energy w.r.t reference	3×10^9
7	Total density (cm^{-3})	1×10^{15}

2.2. Numerical modelling

We have attempted to obtain a numerical expression in our study that links the graphene solar cell's efficiency and the plasma characteristics.
From Ref. [3], we determine the potential across a 2D semiconductor, which is represented as an incredibly thin sheet of thickness h encircled by a dielectric.

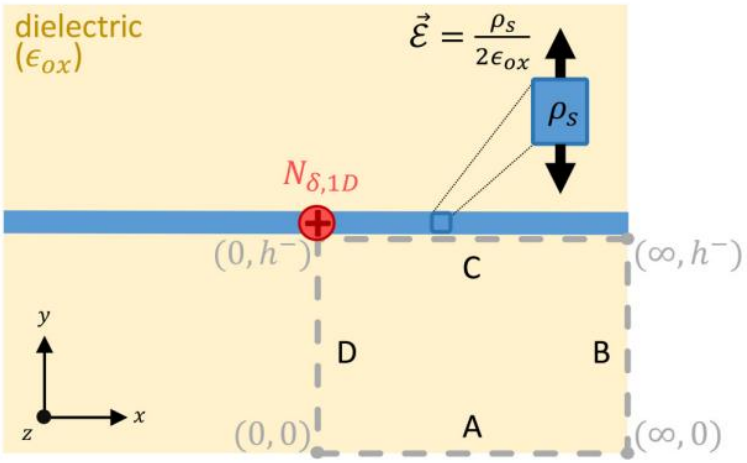

Fig 2.6 Boundary condition for semiconductor sheet [3]

Taking a small line charge perturbation at x=0, we select boundaries at y=0 and y=h. Then $\phi = 0$ is taken as the reference potential. Through application of Gauss law, a relationship between the electric field in the dielectric directly beneath the semiconductor and its charge

density (σ) can be established, [3] and imposing Dirichlet's conditions along the boundaries, we have,

At y = -h,

$$\frac{\partial V}{\partial y} = -E_y = \frac{\sigma}{2\epsilon_{ox}} = \frac{qN_{2D}}{2\varepsilon_{ox}}(1 - \exp(qV/kT)) \tag{2.6}$$

where Ey signifies the electric field in y-direction, ϵ_{ox} is representatie of the dielectric permittivity, q is any point charge, $N_{D,2D}$ is the donor sheet density of 2D semiconductor and kT is the thermal energy.

The net surface charge density, derived from Maxwell Boltzmann approximations, is given by:-

$$\sigma = qN_{2D}\,(1 - \exp(qV/kT)) \tag{2.7}$$

When $q\phi <$ kT, we can linearize the exponential term of equation,

at y = h$^-$

$$\frac{\partial V}{\partial y} = -\frac{q_{N_{2D}}}{2\varepsilon_{ox}}\frac{qV}{kT} \tag{2.8}$$

$$\frac{\partial V}{\partial y} = -\frac{V}{\lambda_D} \tag{2.9}$$

Where the Debye screening length is written as:

$$\lambda_D = \frac{kT}{q}\frac{2\varepsilon_{ox}}{q_{N_{2D}}} \tag{2.10}$$

λ_D is the 2D Debye screening length.

Solving the Poisson's equation $\nabla^2 V = 0$ and following the calculations as done in Ref. [3], we get the general solution which can be written as,

$$V(x,y) = \frac{qN_{1D}}{4\varepsilon_{ox}}\sum_{n=1}^{\infty}\frac{2sin(\lambda_n h)}{\lambda_n(h + cos^2(\lambda_n h)\lambda_D)}\,sin(\lambda_n y)\,e^{-\lambda_n x} \tag{2.11}$$

For y=h we can write,

$$V(x) = V(x, y = h) = \frac{qN_{1D}}{2\varepsilon_{ox}}\sum_{n=1}^{\infty}\frac{(\lambda_n {\lambda_D}^2/h)e^{-\lambda_n x}}{{\lambda_n}^2{\lambda_D}^2 + 1 + \lambda_D/h} \tag{2.12}$$

In the model we let the graphene sheet of length 'l' and thickness 't', put the variables in place of 'x' and 'h' in above expression, we obtain the value of potential across the sheet to be,

(2.13)

$$V(x) = \frac{qN_{2D}}{2\epsilon_{ox}} \sum_{n=1}^{\infty} \frac{(\lambda_n {\lambda_D}^2/h)e^{-\lambda_n l}}{{\lambda_n}^2{\lambda_D}^2 + 1 + \lambda_D/t}$$

We derive the expression for current collected due to positive ions and neutrals from Ref. [6], equation (7) and (8) and take l=0 for 2D graphene sheet.

Taking h → ∞ , the potential is found to be,

$$V' = \frac{eN_{1D}}{2\pi\varepsilon_{ox}} ln(\frac{\lambda_D}{t}) \tag{2.14}$$

where λ_D is the debye length of the plasma given by,

$$\frac{1}{{\lambda_D}^2} = \frac{1}{{\lambda_e}^2} + \frac{1}{{\lambda_i}^2} \tag{2.15}$$

$$\lambda_e = \sqrt{\frac{\varepsilon_o K_B T_e}{n_e e^2}} \ , \lambda_i = \sqrt{\frac{\varepsilon_o K_B T_i}{n_i e^2}} \tag{2.16}$$

And $N_{2D} = N_{1D} \times t_{semiconductor}$

We know the expression for the efficiency for a photovoltaic device is [31],

$$\eta = (\frac{FF \times V_{OC} \times J_{SC}}{P_{inc}}) \tag{2.17}$$

where,

$$V_{OC} = \frac{K_B T}{e} ln(\frac{J_{SC}}{J_O} + 1). \tag{2.18}$$

Taking the ratio of equation (3.1) and (3.5) then substituting in equation (3.4), we get the expression of efficiency in terms of plasma parameters,

$$\eta = (\frac{FF \times J_{SC}}{P_{inc}}) \frac{K_B T N_{1D}}{2\pi\varepsilon_{ox} V} ln(\frac{\lambda_D}{t}) \, ln(\frac{J_{SC}}{J_O} + 1). \tag{2.19}$$

Table 2.4 Parameters used for numerical calculation.

Parameters	Symbol	Value	References
Electron Density	n_e	2.77 x 10^{17} m^{-3}	[50]
Electron Temperature	T_e	2.76 eV	[50]
Ion Density	n_i	5 x 10^{18} m^{-3}	[50]
Ion Temperature	T_i	0.2 eV	[50]
Donor Concentration	N_{2D}	15 x 10^{16} m^{-2}	[3]
Oxide Dielectric Constant	ε_{ox}	$3.9\varepsilon_o$	[3]

CHAPTER 3

RESULTS & CONCLUSION

3.1. Results & Discussion

Band gap diagram of the simulated model

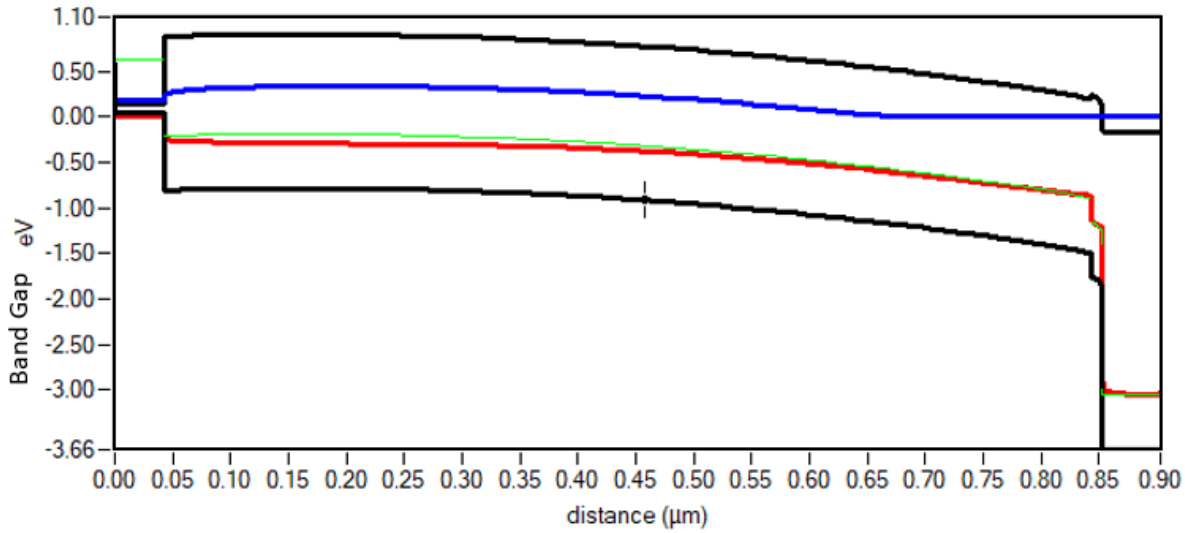

Fig. 3.1 Bang gap diagram of the simulated GrPrSC model.

Fig 3.1 shows the band gap structure of the GrPrSC model. The above illustration shows various layers of the solar cell derived from SCAPS- 1D software. It lets us analyse the performance the solar cell.

Examining the variation of quantum efficiency with absorber thickness observed in the simulated model

The quantity known as quantum efficiency Q_{eff} indicates "how many electron hole pairs are produced for every incident photon"[49]. The spectra gives us a measure of the total solar energy absorbed by the device. It gives all the information about the photon, whether it is reflected, absorbed or transmitted. **Fig 3.2**. depicts the plot of how the quantum efficiency changes when there is a noticeable variation in the wavelength of the incident light.

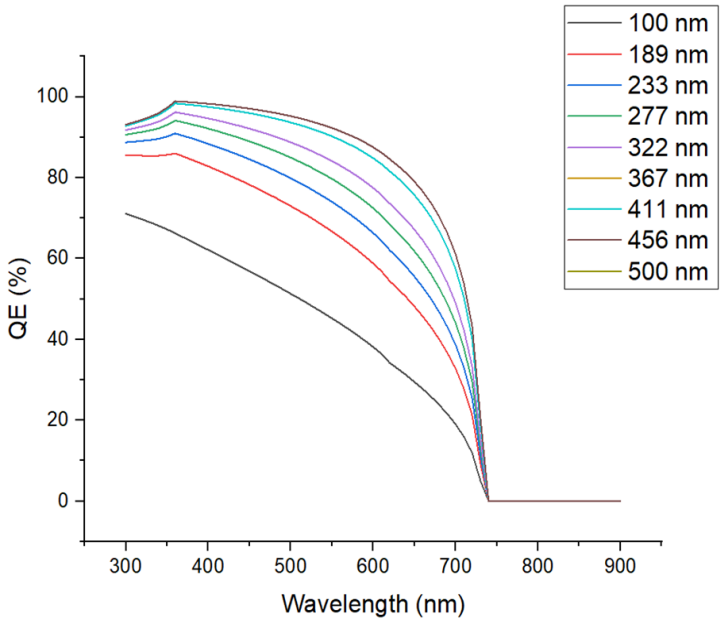

Fig. 3.2 Plot of change in Q_{eff} with a varying values of the incident wavelength.

Variation analysis of the J-V Characteristics with changing values of absorber thickness.

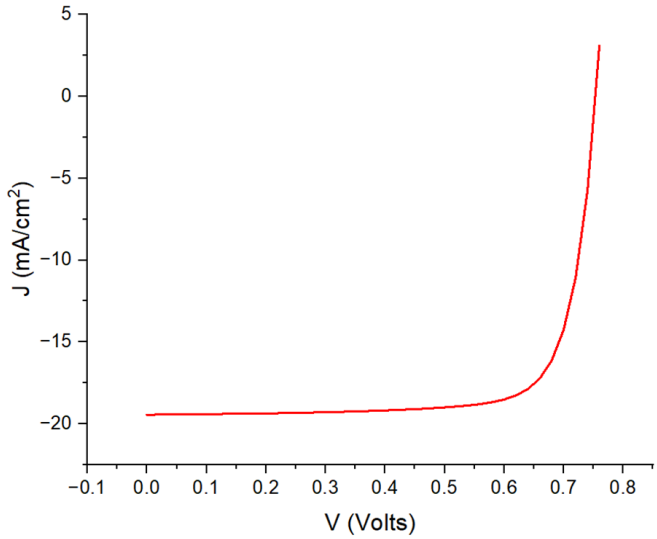

Fig. 3.3 The J-V curve for the graphene based solar cell when absorber thickness is 500 nm.

One essential tool we use to "evaluate the performance of a solar cell" is the J-V curve. It provides significant information about the apparatus's electrical characteristics. The J-V curve can also tell us about the device's PCE_{ff}. **Fig 3.3** displays the J-V curve for the simulated GrPrSC model at 500 nm thickness of the $CsPbI_3$ layer. The production of positively and negatively charged carriers known as holes and electrons is triggered by photons that land on the surface of the solar cell at AM 1.5. The photocurrent that the photovoltaic device produces is the result of these electron-hole pairs.

More current is generated when we increase the thickness of the absorber layer. In this work, we varied the thickness of the absorber layer between 100 and 1000 nm to improve the device efficiency.

The simulated results are in accordance with the research previously done.

Variation analysis of solar cell parameters using simulated absorber thickness using SCAPS-1D software.

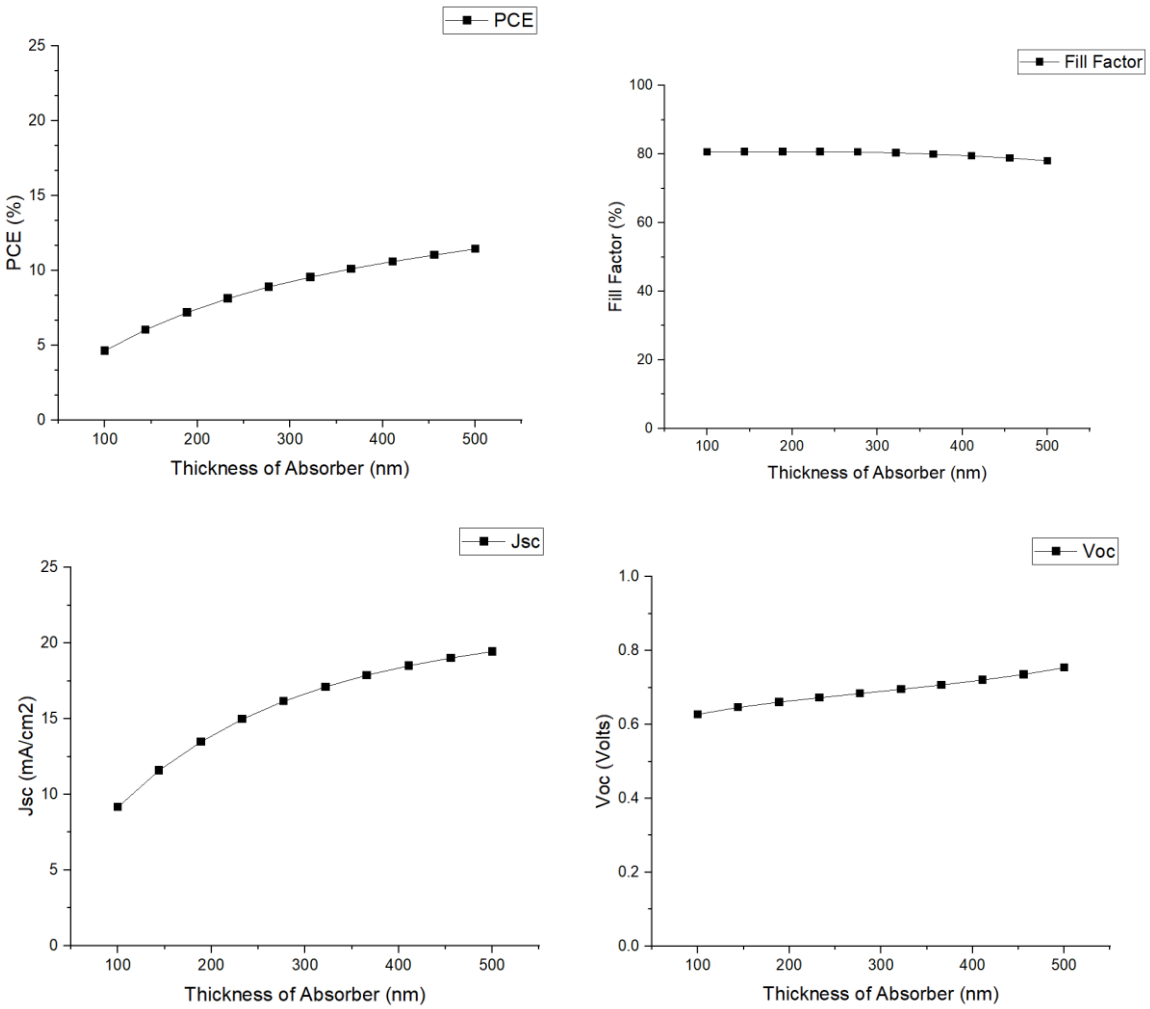

Fig. 3.4 These plots show the various trends with J_{sc}, $PCE_{eff.}$, FF, V_{oc} when the absorber is varied from 100 nm thick to 500 nm thick.

As observed from the fig 3.5, the $PCE_{ff.}$ and J_{sc} show a steady increase if we increase the absorber ($CsPbI_3$) thickness while fill factor FF shows a constant trend. This is because of the increase in V_{oc} as observed above in the figure. The curves of efficiency ($PCE_{ff.}$) shoot upwards and J_{sc} start to saturate around 500 nm, indicating that any further introduction of increment in thickness of absorber will lead to no changes in the J_{sc} of the simulated GrPrSC device. From **Fig 3.4**, the increase in efficiency η shows that with an increasing thickness of absorber, more incident light gets absorbed leading to a higher current generation and increased device efficiency as observed. However, the light absorption reaches a maximum after a certain thickness and any further increment in the thickness leads to no further changes in the GrPrSC efficiency and the current density. The FF of the simulated devices shows an almost constant trend line, with an incredibly small decrease around 700 nm, as observed from the figure, and V_{oc} shows an increasing trend when we introduce an increment in the absorber ($CsPbI_3$) thickness. From the J-V curve, at 500 nm thick $CsPbI_3$ layer, we obtain a $PCE_{ff.}$ of 11.442%, a FF of around 78.0518 %, J_{sc} around 19.4428 mA/cm^2 and V_{oc} near the value 0.754 V.

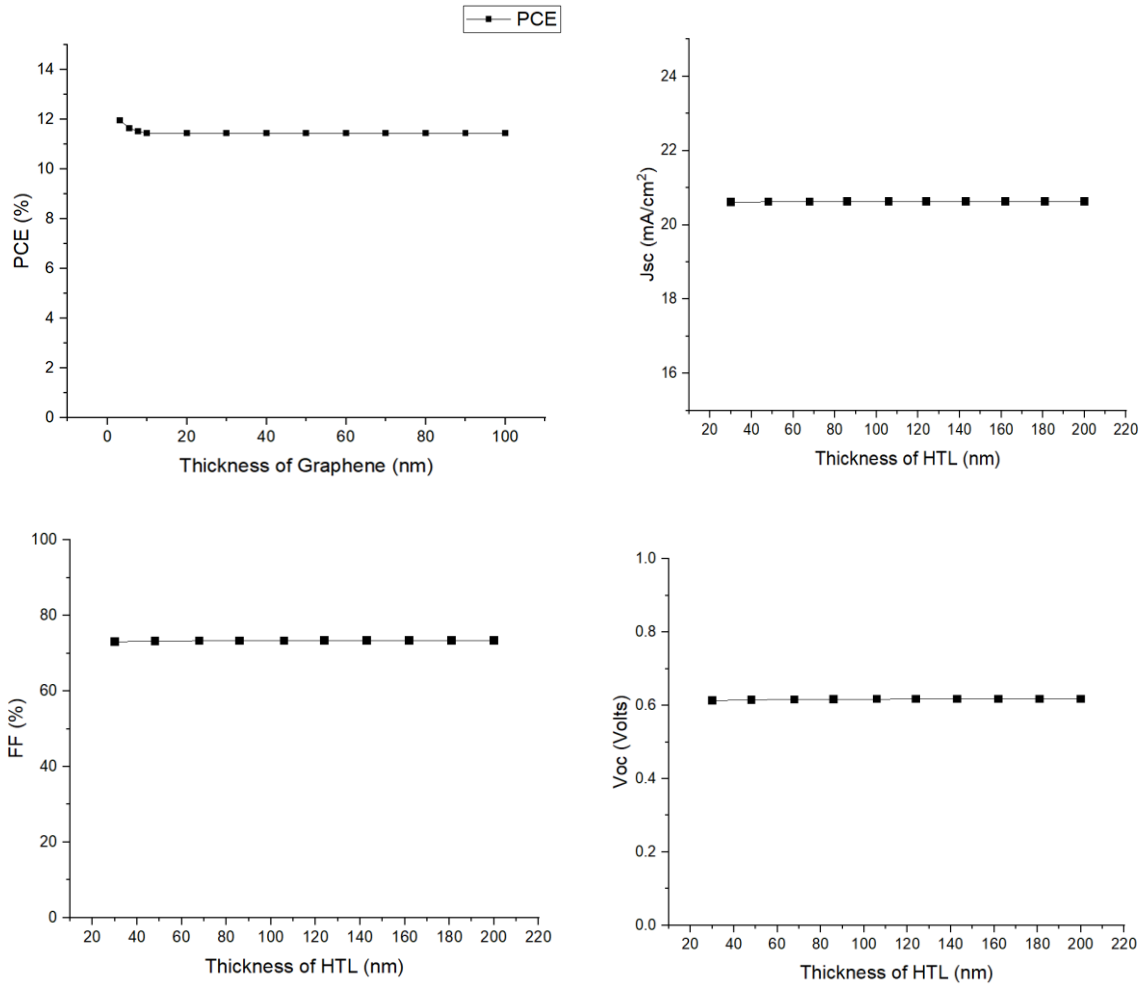

Fig. 3.5 A constant trend with $PCE_{ff.}$, J_{sc}, FF, V_{oc} is shown when HTL thickness is changed.

Fig 3.5 shows how important paramters of solar cell which describe its working and properties varies graphically with the thickness of HTL (plasma assisted graphene). Not much impact of the HTL replaced by graphene is seen on J_{sc} and shows values ranging from 19.448 mA/cm^2 to 19.449 mA/cm^2 . Similar trend for FF is observed as shown in the graph. V_{oc} is shown to range from 0.753823 V to 0.758532 V. The trends shown in the results are in compliance with the research done previously. [59]-[76].

Summarized results from SCAPS- 1D simulation

Table 3.1 Variation in solar cell parameters with changing thickness of absorber layer

Thickness of Absorber (nm)	V_{OC} (V)	J_{SC} (mA/cm^2)	FF (%)	Efficiency (%)
100	0.627589	9.162042	80.6287	4.6362
144	0.64621	11.58848	80.7404	6.0463
189	0.660747	13.48206	80.7311	7.1917
233	0.672549	14.97424	80.7223	8.1295
277	0.684017	16.16085	80.5752	8.907
322	0.695214	17.11258	80.3495	9.5591
366	0.707091	17.88222	80.0009	10.1156
411	0.72059	18.50929	79.488	10.6018
456	0.735714	19.02375	78.8631	11.0377
500	0.753823	19.44828	78.0518	11.4428

Table 3.2 Variation in solar cell parameters with changing thickness of HTL layer

Thickness of HTL (nm)	V_{OC} (V)	J_{SC} (mA/cm^2)	FF (%)	Efficiency (%)
10	0.753823	19.44828	78.0518	11.4428
20	0.753847	19.44829	78.0522	11.4433
30	0.753823	19.44828	78.0518	11.4428
40	0.753825	19.44828	78.0519	11.4429
50	0.753827	19.44828	78.0519	11.4429
60	0.753828	19.44828	78.0519	11.4429
70	0.75383	19.44828	78.052	11.443
80	0.753832	19.44828	78.052	11.443
90	0.753833	19.44828	78.052	11.443
100	0.753834	19.44828	78.052	11.443

Comparison between results obtained from simulation of solar cell model in SCAPS – 1D and the results calculated numerically

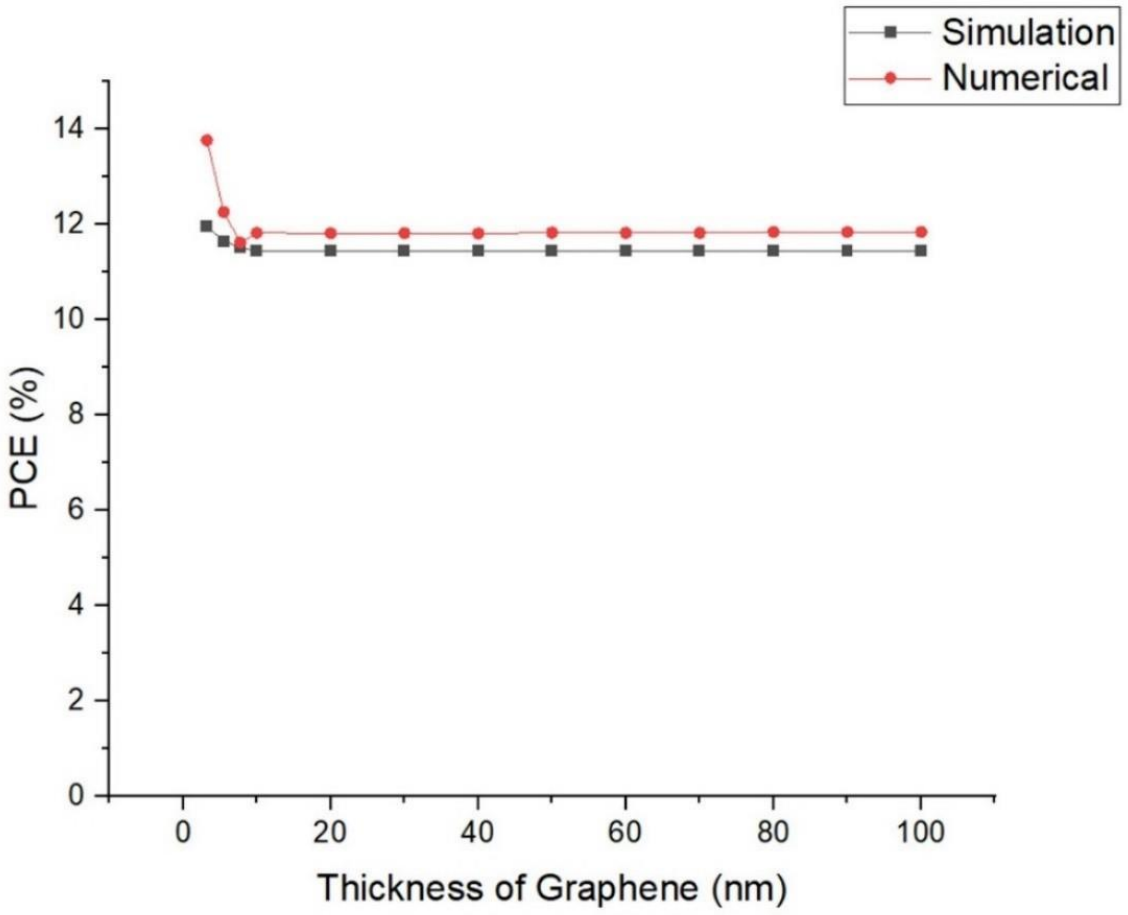

Fig. 3.6 A comparative plot between the how the graphene thickness (which serves as the HTL) affects the efficiency calculated for the simulated model and calculated numerically.

The **Fig 3.6** demonstrates a comparison between the efficiency fluctuation with graphene thickness found by numerical and simulation methods. The PCEff., which is computed numerically and for the simulated model, decreases slightly from 3.25 nm to 10 nm until the graph saturates, showing that additional thickness modifications have no effect on the PCEff. The cause might be traced to a number of environmental variables, including variations in the amount of sun radiation and the temperature at which the device is being used. This outcome is consistent with the study conducted by Sagar Bhattarai et al [39]. Because graphene is a two-dimensional material, its electronic characteristics are limited to its plane. Its ability to perform its job and play a part in charge transport is not greatly altered by adding more layers. Graphene can create a layer that is devoid of defects and offers efficient surface covering even at the lowest thickness. Unlike other materials, graphene exhibits chemical stability and resistance to deterioration, resulting in consistent efficiency despite variations in thickness. The efficiency's invariance with HTL thickness permits flexibility in the film's manufacture process. Graphene can be deposited as HTL by manufacturers without the requirement for exact thickness control.

The simulated model yields a result where the $PCE_{ff.}$ of 11.442%, a FF of around 78.0518 %, J_{sc} around 19.4428 mA/cm^2 and V_{oc} near the value 0.754 V at an optimum thickness of 33.4 nm. The numerical results for the same FF, J_{sc}, V_{oc} and thickness shows a $PCE_{ff.}$ of 11.84%.

Table 3.3 Comparison between the results obtained from simulation and numerical modelling

Thickness of HTL (nm)	V_{OC} (V)	J_{SC} (mA/cm^2)	FF (%)	Simulated Efficiency (%)	Numerical Efficiency (%)
5.5	0.765328	19.45181	78.2628	11.651	12.2628
7.75	0.758532	19.44971	78.1201	11.5252	11.62199
10	0.753823	19.44828	78.0518	11.4428	11.82573
20	0.753847	19.44829	78.0522	11.4433	11.81532
33.4	0.753823	19.44828	78.0518	11.4428	11.82138
40	0.753825	19.44828	78.0519	11.4429	11.811
50	0.753827	19.44828	78.0519	11.4429	11.82743
90	0.753833	19.44828	78.052	11.443	11.84018
100	0.753834	19.44828	78.052	11.443	11.8402

Analysis of impact of plasma parameters on the Solar Cell parameters particularly efficiency

Now we analyze the impact of plasma parameters on the device photovoltaic parameters particularly efficiency. Table 9 lists the various parameters used in the simulation of the trendlines shown in the graphs below. (**Fig 3.7**, **Fig 3.8**, **Fig 3.9**, **Fig 3.10**).

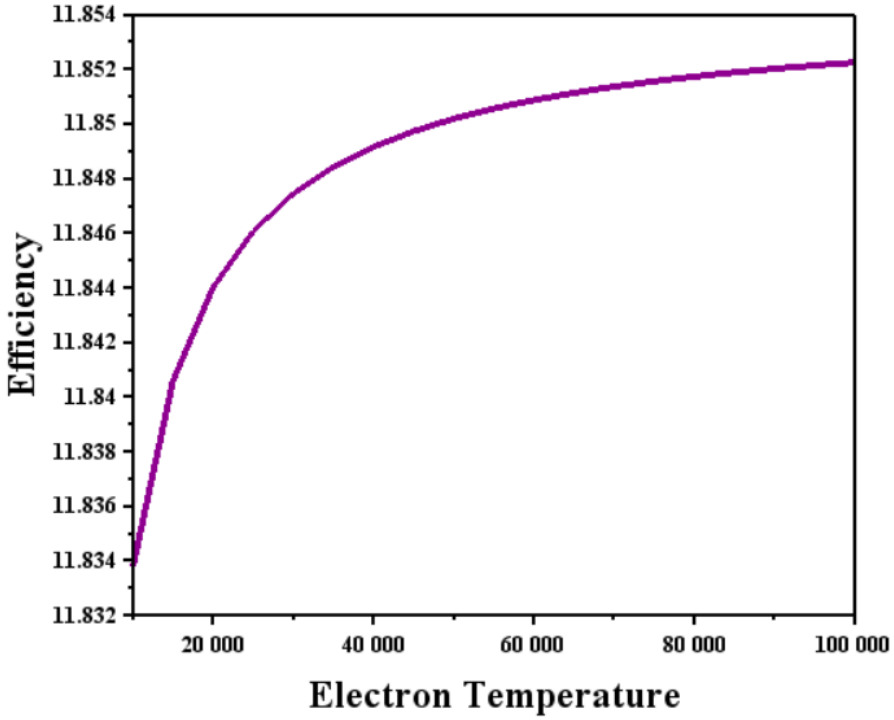

Fig. 3.7 $PCE_{ff.}$ enhances when an increment is introduced in T_e.

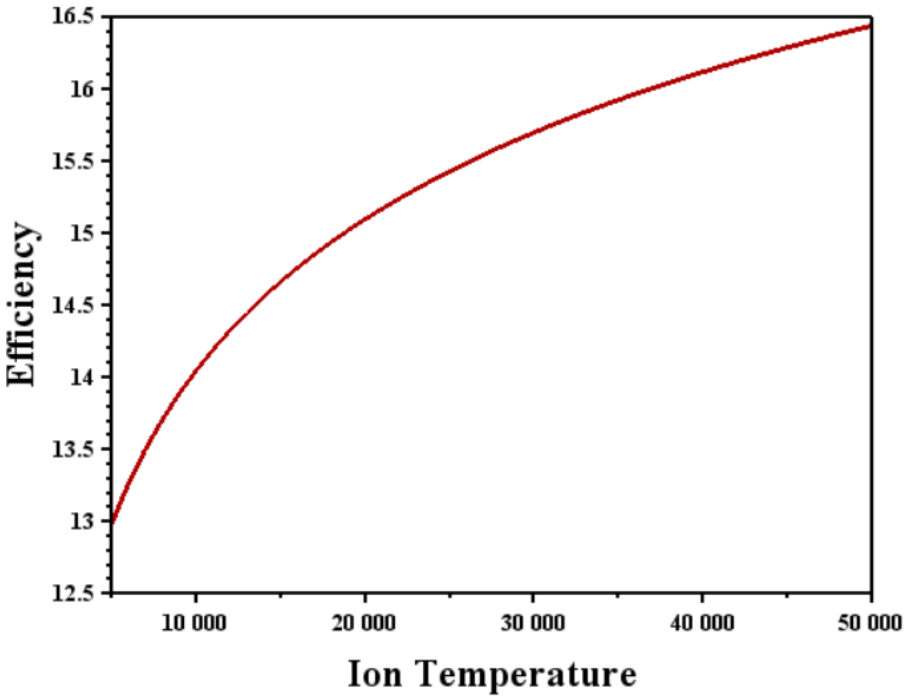

Fig. 3.8 PCE_{ff}. is enhanced when an increment is introduced in T_i.

From **Fig 3.7** and **Fig 3.8**, we can observe a direct relationship between T_e and T_i and the PCE_{ff}. of the device. The reason for this can be attributed to the fact that the debye length λ_D directly proportional to T_e and T_i and hence has an overall impact upon the results. Hence the graph shows that upon decreasing the T_e and T_i, the PCE_{ff}. of the device increases.

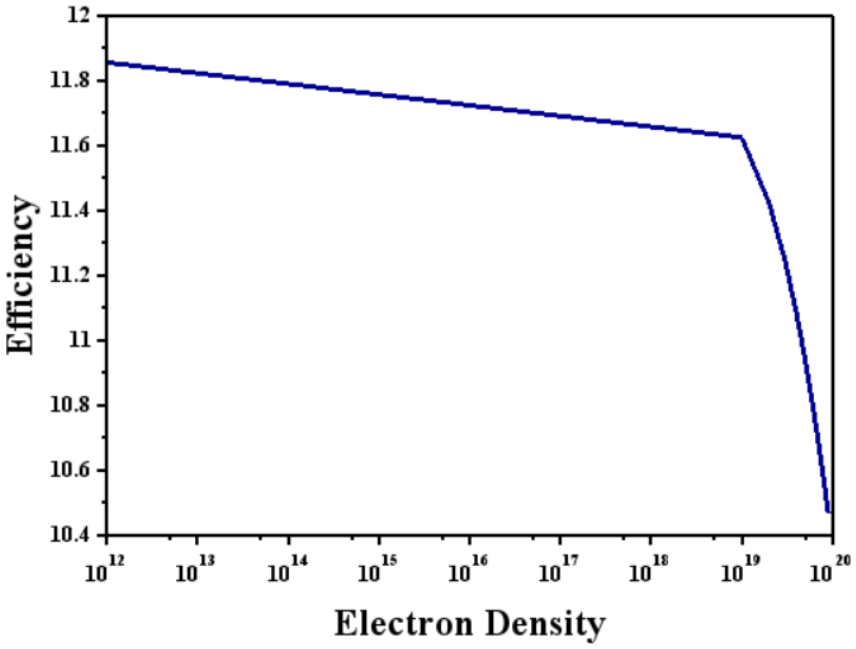

Fig. 3.9 PCE_{ff}. reduces when an increment is introduced in n_e

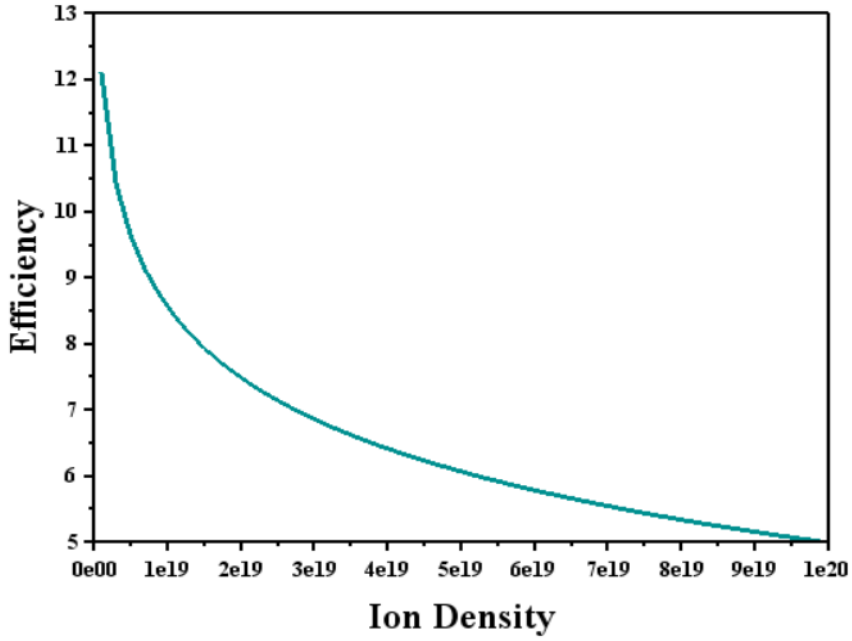

Fig. 3.10 PCE_{ff}. shows an inverse relation with the ion density n_i

Similarly, n_e and n_i are inversely proportional to the debye length λ_D, leading to an inverse relation with the efficiency resulting in the trends as shown in **Fig 3.9** and **Fig 3.10**.

The **Fig 3.7** – **Fig 3.10** shows the variation trendlines between efficiency of device and plasma parameters (n_e, n_i, T_e, T_i) calculated numerically using the values given in **Table 2.4**, at an optimum thickness of 33.4 nm, where a FF = 78.0518 %, J_{sc} = 19.4428 mA/cm^2 and V_{oc} = 0.754 V is taken.

Low carrier lifetimes, high defect density, and low recombination rates can all be prevented by maintaining ideal plasma conditions. These plasma conditions also affect the interface's sharpness. Device efficiency can be reduced by a poor interface. The device's efficiency is directly impacted by variations in the ratio of t/λ_D and the ensuing 2D debye screening effect, as demonstrated by **Eqs 2.19**. This was established during the numerical modeling of the device.

Since the electron density n_e is inversely proportional to the debye length λ_D, it leads to an inverse relation with the efficiency. Higher density of electrons and ions results in increased collisions and defects. It can also cause rapid growth rates and non uniformity in the graphene layer. Non uniformity affects the electrical conductivity of the device and hence affects the device efficiency. On the other hand the electron temperature is directly proportional to the debye length λ_D, leading to a direct relation with the efficiency and hence resulting in the trends as shown in **Fig 3.7 – Fig 3.10.** This could be due to the enhanced reaction kinetics from the increased T_e, leading to formation of higher quality graphene as well as cleaner substrate prior to graphene growth which can help in reducing defects and recombination and improving crystalline quality in the film. Therefore a balance between the T_e and n_e is necessary to produce high quality graphene sheets that enhances the efficiency of the GrPrSC.

Table 3.4 Summary of the analysis of the impact of plasma parameters on the device efficiency

S.N.	Parameter	Effect on the Solar Cell Efficiency
1	Electron Temperature T_e	Increases with an increase in T_e and λ_D
2	Ion Temperature T_i	Increases with an increase in T_i and λ_D
3	Electron Density n_e	Decreases with an increases in n_e and λ_D
4	Ion Temperature n_i	Decreases with an increase in n_i and λ_D

3.1. Conclusion

An efficiency of 11.442 % is achieved along with an FF = 78.0518 %, J_{sc} = 19.4428 mA/cm^2 and V_{oc} = 0.754 V when a 33,4 nm thick graphene and 790 nm thick $CsPbI_3$ which here serves as the absorber is taken in a model of ITO/PCBM/$CsPbI_3$/Graphene is simulated using SCAPS-1D. Taking the same values from the simulated model and incorporating them in our formula, we deduce the numerical efficiency to be 11.84 %. If we increase the electron and ion densities, we observe an inverse relation with the efficiency which decreases steadily. Similarly, upon increasing the electron and ion temperatures the trend of efficiency gives us a direct relation with the parameters and increases. Therefore, we conclude that manipulation of the PoCE of a GrPeSC is possible by changing the $CsPbI_3$ thickness and parameters of the plasma used to grow the graphene sheet.

3.2. Future Scope

1. Graphene is a great material for solar cells because of its remarkable electrical conductivity and transparency. Increasing the ratio of graphene to other materials can result in more efficient devices.

2. Large-scale, highly-efficient, and scalable manufacturing of high-quality graphene is possible with the PECVD technique.

3. The chemical stability and mechanical strength of graphene add to the long-term performance and resilience of solar cells.

4. Moreover, graphene is not easily degraded by the atmosphere. The environmental effect of solar cell manufacturing can be further reduced by developing ecologically benign precursors for graphene production and improving the PECVD process.

5. Developing scalable and economical production techniques, integrating graphene with other materials, and guaranteeing reliable, high-quality graphene production are a few of the difficulties.

References

[1]. Lewis Fraas, Larry Partain, *Solar Cells and their Applications.*

[2]. F.F. Chen, *Introduction to Plasma Physics and Controlled Fusion*.

[3]. Adina R. Bechhofer*,* Akiko Ueda, Ankur Nipane, James T. Teherani. The 2D Debye Length: An analytical study of weak charge screening in 2D Semiconductors*, J. Appl. Phys,* **129**, 024301 (2021).

[4]. Malik Abdul Rehman, Sanjib Baran Roy, Imtisal Akhtar, Muhammad Fahad Bhopal, Woosuk Choi, Ghazanfar Nazir, Muhammad Farooq Khan, Sunil Kumar, Jonghwa Eom, Seung-Hyun Chun, Yongho Seo*,* Thickness-dependent efficiency of directly grown graphene based solar cells, *Carbon*, 148 (2019) 187-195.

[5]. Suresh C. Sharma**,** Neha Gupta*,* Theoretical modeling of the plasma-assisted catalytic growth and field emission properties of graphene sheet*, Physics of Plasmas,* 22*,* 123517 (2015); doi: 10.1063/1.4938506.

[6]. N. Gupta, R. Gupta, S. C. Sharma, Investigations on the effect of process parameters on the growth of vertically oriented graphene sheet in plasma-enhanced chemical vapour deposition system, *Contributions to Plasma Physics,* 2021, e202100069.

[7]. Muhammad Zahir Iqbal, Assad-Ur Rehman, Recent progress in Graphene incorporated Solar Cell Devices, *Solar Energy*, 169 (2018) 634–647.

[8]. M. A. Lieberman and A. J. Lichtenberg*, Principles of Plasma Discharges and Materials Processing (Wiley Interscience Publication, USA)*.

[9]. Muhammad Ali, Amir Muhammad Afzal, Muhammad Waqas Iqbal, Sohail Mumtaz, Muhammad Imran, Faria Ashraf, Asad Ur Rehman, Faqeer Muhammad, *2D-TMDs based electrode material for supercapacitor applications,* https://doi.org/10.1002/er.8698.

[10]. Xuefen Song, Jian Liu, Leyong Yu, Jun Yang, Liang Fang, Haofei Shi, Chunlei Du, Dapeng Wei, Direct versatile PECVD growth of graphene nanowalls on multiple substrate, *Materials Letters*, 137 (2014) 25–28.

[11]. Malik Abdul Rehman, Sanjib Baran Roy, Dham Gwak, Imtisal Akhtar, Naila Nasir, Sunil Kumar, Muhammad Farooq Khan, Kwang Heo, Seung-Hyun Chun, Yongho Seo, Solar cell based on vertical graphene nano hills directly grown on silicon*, Carbon,* 164 (2020) 235-243.

[12]. Gary Hodes, Prashant V. Kamal, Understanding the Implication of Carrier Diffusion Length in Photovoltaic Cells*, J. Phys. Chem. Lett*, 2015, 6, 4090−4092.

[13]. Liangchao Guo, Zhenyu Zhang, Hongyan Sun, Dan Dai, Junfeng Cui, Mingzheng Li, Yang Xu, Mingsheng Xu, Yuefeng Du, Nan Jiang, Feng Huang, Cheng-Te Lin, Direct formation of wafer-scale single-layer graphene films on the rough surface substrate by PECVD*, Carbon,* 129 (2018) 456-461.

[14]. Yiqian Cui, Jiaqi Wei1, Lizhe Jia*,* Defect-minimized directly grown graphene-based solar cells, *Materials Science-Poland*, 40(3), 2022, pp. 125-134.

[15]. Martin Bivour, Sebastian Schröer, Martin Hermle, Numerical analysis of electrical TCO / a-Si:H(p) contact properties for silicon heterojunction solar cells, *Energy Procedia,* 38 (2013) 658 – 669.

[16]. R. J. Kortschot, A. P. Philipse, B. H. Erne, Debye Length Dependence of the Anomalous Dynamics of Ionic Double Layers in a Parallel Plate Capacitor, *J. Phys. Chem*. C 2014, 118, 11584−11592.

[17]. Zongyou Yin , Jixin Zhu , Qiyuan He , Xiehong Cao , Chaoliang Tan , Hongyu Chen , Qingyu Yan , and Hua Zhang, Graphene-Based Materials for Solar Cell Applications*, Adv. Energy Mater*. 2014, 4, 1300574.

[18]. L. Chandana, Partha Ghosal, Subrahmanyam Challapalli, Improved Solar Cell Performance of High Quality Plasma Reduced Graphene Oxide*, Plasma Process*. Polym. 2016,

[19]. Neha Gupta and Suresh C. Sharma, Effect of gas composition on morphological properties of graphene nanosheet, *Physics of Plasmas* 24, 073510 (2017).

[20]. M. Burgelman, P. Nollet and S. Degrave, "Modelling polycrystalline semiconductor solar cells", *Thin Solid Films*, 361-362, 527-532 (2000).

[21]. M. Burgelman, K. Decock, S. Khelifi and A. Abass, "Advanced electrical simulation of thin film solar cells", *Thin Solid Films*, 535 (2013) 296-301.

[22]. K. Decock, P. Zabierowski, M. Burgelman, "Modeling metastabilities in chalcopyrite-based thin film solar cells", *Journal of Applied Physics*, 111 (2012) 043703.

[23]. K. Decock, S. Khelifi and M. Burgelman, "Modelling multivalent defects in thin film solar cells", *Thin Solid Films*, 519 (2011) 7481-7484.

[24]. M. Burgelman and J. Marlein, "Analysis of graded band gap solar cells with SCAPS", *Proceedings of the 23rd European Photovoltaic Solar Energy Conference*, (Valencia, E, september 2008), 2151-2155, (2008).

[25]. J. Verschraegen and M. Burgelman, "Numerical modeling of intra-band tunneling for heterojunction solar cells in SCAPS", *Thin Solid Films*, 515 (15), 6276-6279 (2007).

[26]. S. Degrave, M. Burgelman, P. Nollet, "Modelling of polycrystalline thin film solar cells: new features in SCAPS version 2.3", *Proceedings of the 3rd World Conference on Photovoltaic Energy Conversion* (Osaka, Japan, may 2003), pp. 487-490, WCPEC-3, Osaka, 2003.

[27]. A. Niemegeers and M. Burgelman, "Numerical modelling of ac-characteristics of CdTe and CIS solar cells", *Proc. 25nd IEEE Photovol-taic Specialists Conference* (Washington D.C., april 1996), pp. 901-904, IEEE, New-York, 1996.

[28]. Tasnimul Islam Taseen, M. Julkarnain, Abu Zafor Md Touhidul Islam, Design and simulation of nitrogenated holey graphene (C2N) based heterostructure solar cell by SCAPS-1D, *Heliyon* 10 (2024) e23197.

[29]. M. Khalid Hossain, Mirza Humaun Kabir Rubel, G. F. Ishraque Toki, Intekhab Alam, Md. Ferdous Rahman, and H. Bencherif, Effect of Various Electron and Hole, Transport Layers on the Performance of $CsPbI_3$-Based Perovskite Solar Cells: A Numerical Investigation in DFT, SCAPS-1D, and wxAMPS Frameworks, *ACS Omega* 2022, 7, 43210−43230,

[30]. M. Shihab Uddin, M. Khalid Hossain, Md Borhan Uddin, Gazi F. I. Toki, Mohamed Ouladsmane, Mirza H. K. Rubel, Daria I. Tishkevich, P. Sasikumar, Rajesh Haldhar, and Rahul Pandey, An In-Depth Investigation of the Combined Optoelectronic and Photovoltaic Properties of Lead-Free Cs2 AgBiBr6 Double Perovskite Solar Cells Using DFT and SCAPS-1D Frameworks, *Adv. Electron. Mater*. 2024, 2300751

[31]. Nabarun Saha , Giuseppe Brunetti , Mario N. Armenise , Aldo Di Carlo ,and Caterina Ciminelli, Modeling Highly Efficient Homojunction Perovskite Solar Cells With Graphene-TiO2 Nanocomposite as the Electron Transport Layer, *IEEE Journal Of Photovoltaics, Vol*. 13, No. 5, Septemeber 2023

[32].K.I. Bolotin, K.J. Sikes, Z. Jiang, M. Klima, G. Fudenberg, J. Hone, P. Kim, H.L.Stormer, Ultrahigh electron mobility in suspended graphene, *Solid State Commun*. 146, 351-355 (2008).

[33]. R.R Nair, P. Blake, A. N. Grigoreniko, K. S. Novoselov, T. J. Booth, T. Stauber, N. M. R. Peres, A. K. Geim, Fine Structure Constant Defines Visual Transparency of Graphene *Science* 320,1308 (2008).

[34]. Alexander. A. Balandin, Suchismita Ghosh, Wenzhong Bao, Irene Calizo, Desalegne Teweldebrhan, Feng Miao, Chun Ning Lau, Superior Thermal Conductivity of Single – Layer Graphene, *Nano Lett*. 8, 902-907 (2008)

[35]. Eric Ganz, Ariel B. Ganz, Li-Ming Yang, Matthew Dornfeld, The initial stages of melting of graphene between 4000 K and 6000 K, *Phys. Chem. Chem. Phys*. 19, 3756-3762 (2017).

[36]. Na Li, Zhen Zhen, Rujing Zhang, Zhenhua Xu, Zhen Zheng, Limin He. Nucleation and growth dynamics of graphene grown by radio frequency plasma-enhanced chemical vapor deposition. *Sci Rep 11*, 6007 (2021).

[37]. Chang-Soo Park, Heetae Kim, Variation of Band Gap in Graphene Grown by Plasma Enchanced Chemical Vapor Deposition, *Annals of Chemical Science Research*, 000529. 2(1).2020.

[38]. Mohammed M. Shabat, Guillaume Zoppi, Simulation on the perovskite-based solar cell with graphene derivative, The 8th International Engineering Conference on Renewable Energy & Sustainability, 2023.

[39]. Sagar Bhattarai, M. Khalid Hossain, Rahul Pandey, Jaya Madan, D.P. Samjdar, Mithun Chowdhury, Md. Ferdous Rahman, Mohd Zahid Ansari, Munirah D. Albaqami, Enhancement of efficiency in C_sSnI_3 based perovskite solar cell by numerical modeling of graphene oxide as HTL and ZnMgO as ETL, *Heliyon*, 10 (2024) e24107.

[40]. Eperon, G. E; Paterno, G. M.; Sutton, R. J.; Zampetti, A.; Haghighirad, A. A.; Cacialli, F.; Snaith, H. J. Inorganic Caesium Lead Iodide Perovskite Solar Cells. *J. Mater. Chem.* A 2015, 3, 19688-19695.

[41]. Abdelaziz, S.; Zekry, A.; Shaker, A.; Abouelatta, M., Investigating the Performance of Formamidinium Tin-Based Perovskite Solar Cell by SCAPS Device Simulation. *Opt. Mater.* 2020, *101*, 109738.

[42]. Anwar, F.; Afrin, S.; Satter, S. S.; Rafee Mahbub, S. M. U. Simulation and Performance Study of Nanowire CdS/CdTe Solar Cell. *Int. J. Renew. Energy Res.* 2017, v7i2.

[43]. Moon, M. M. A.; Ali, M. H.; Rahman, M. F.; Kuddus, A.; Hossain, J.; Ismail, A. B. M. Investigation of Thin-Film p -BaSi2/n-CdS Heterostructure towards Semiconducting Silicide Based High Efficiency Solar Cell. *Phys. Scr.* 2020, *95*, No. 035506.

[44]. Jayan, K. D.; Sebastian, V.; Kurian, J. Simulation and Optimization Studies on $CsPbI_3$ Based Inorganic Perovskite Solar Cells. *Sol. Energy* 2021, *221*, 99−108.

[45]. Gan, Y.; Bi, X.; Liu, Y.; Qin, B.; Li, Q.; Jiang, Q.; Mo, P. Numerical Investigation Energy Conversion Performance of Tin-Based Perovskite Solar Cells Using Cell Capacitance Simulator, *Energies* 2020, *13*, 5907.

[46]. Singla, A.; Pandey, R.; Sharma, R.; Madan, J.; Singh, K.; Yadav, V. K.; Chaujar, R.Numerical Simulation of CeOx ETL Based Perovskite Solar Cell:- An Optimization Study for High Efficiency and Stability. In *2018 IEEE Electron Devices Kolkata Conference (EDKCON)*; IEEE, *2018*; pp. 278−282. DOI: 10.1109/EDKCON.2018.8770401.

[47]. Lakhdar, N.; Hima, A. Electron Transport Material Effect on Performance of Perovskite Solar Cells Based on $CH_3NH_3GeI_3$. *Opt. Mater.* 2020, *99*, 109517.

[48]. Muhammed Zahir Iqbal, Assad- Ur Rehman, Recent progress in graphene incorporated solar cell devices, *Solar Energy,* 169 (2018) 634–647

[49]. M. Khalid Hossain, D.P. Samajdar, Ranjit C. Das, A. A. Arnab, Md. Ferdous Rahman, M. H. K. Rubel, Md. Rasidul Islam, H. Bencherif, Rahul Pandey, Jaya Maden, Mustafa K. A. Mohammed, Design and Simulation of Cs2BiAgI6 Double Perovskite Solar Cells with Different Electron Transport Layers for Efficiency Enhancement, *Energy Fuels*, 2023, 37, 3957-3979

[50]. Neha Gupta, Ravi Gupta, Suresh C. Sharma, Investigations on the effect of process parameters on the growth of vertically oriented graphene sheet in plasma-enhanced chemical vapour deposition system, *Contrib. Plasma Phys*. 2021; e202100069. https://doi.org/10.1002/ctpp.202100069

[51]. Tasnimul Islam Taseen, M. Julkarnain, Abu Zafor Md Touhidul Islam, Design and simulation of nitrogenated holey graphene (C2N) based heterostructure solar cell by SCAPS-1D, *Heliyon* 10 (2024) e23197. https://doi.org/10.1016/j.heliyon.2023.e23197

[52]. M. Shihab Uddin, M. Khalid Hossain, Md Borhan Uddin, Gazi F. I. Toki, Mohamed Ouladsmane, Mirza H. K. Rubel, Daria I. Tishkevich, P. Sasikumar, Rajesh Haldhar, and Rahul Pandey, An In-Depth Investigation of the Combined Optoelectronic and Photovoltaic Properties of Lead-Free Cs2 AgBiBr6 Double Perovskite Solar Cells Using DFT and SCAPS-1D Frameworks, *Adv. Electron. Mater*. 2024, 2300751. https://doi.org/10.1002/aelm.202300751

[53]. Nabarun Saha , Giuseppe Brunetti , Mario N. Armenise , Aldo Di Carlo ,and Caterina Ciminelli, Modeling Highly Efficient Homojunction Perovskite Solar Cells With Graphene-TiO2 Nanocomposite as the Electron Transport Layer, *IEEE Journal Of Photovoltaics, Vol*. 13, No. 5, Septemeber 2023. DOI:10.1109/JPHOTOV.2023.3289574

[53].K.I. Bolotin, K.J. Sikes, Z. Jiang, M. Klima, G. Fudenberg, J. Hone, P. Kim, H.L.Stormer, Ultrahigh electron mobility in suspended graphene, *Solid State Commun*. 146, 351-355 (2008). https://doi.org/10.1016/j.ssc.2008.02.024

[54]. R.R Nair, P. Blake, A. N. Grigoreniko, K. S. Novoselov, T. J. Booth, T. Stauber, N. M. R. Peres, A. K. Geim, Fine Structure Constant Defines Visual Transparency of Graphene, *Science* 320,1308 (2008). DOI: 10.1126/science.1156965

[55]. Alexander. A. Balandin, Suchismita Ghosh, Wenzhong Bao, Irene Calizo, Desalegne Teweldebrhan, Feng Miao, Chun Ning Lau, Superior Thermal Conductivity of Single – Layer Graphene, *Nano Lett*. 8, 902-907 (2008). DOI: 10.1021/nl0731872

[56]. Eric Ganz, Ariel B. Ganz, Li-Ming Yang, Matthew Dornfeld, The initial stages of melting of graphene between 4000 K and 6000 K, *Phys. Chem. Chem. Phys*. 19, 3756-3762 (2017). https://doi.org/10.1039/C6CP06940A

[57]. Na Li, Zhen Zhen, Rujing Zhang, Zhenhua Xu, Zhen Zheng, Limin He. Nucleation and growth dynamics of graphene grown by radio frequency plasma-enhanced chemical vapor deposition. *Sci Rep 11*, 6007 (2021). https://doi.org/10.1038/s41598-021-85537-3

[58]. Burgelman, M.; Nollet, P.; Degrave, S. Modelling Polycrystal-line Semiconductor Solar Cells, *Thin Solid Films,* 2000, 361-362, 527−532

[59]. S. Mekhilef, R. Saidur, A. Safari, A review on solar energy use in industries, Renew. Sustain. Energy Rev. 15 (4) (2011) 1777–1790. DOI: 10.1016/j.rser.2010.12.018

[60]. Ehrler, B.; Alarcón-Lladó, E.; Tabernig, S. W.; Veeken, T.; Garnett, E. C.; Polman, A. Photovoltaics Reaching for the Shockley–Queisser Limit. ACS Energy Lett. 2020, 5, 3029– 3033, DOI: 10.1021/acsenergylett.0c01790

[61]. Hossain, M. K.; Pervez, M. F.; Tayyaba, S.; Uddin, M. J.; Mortuza, A. A.; Mia, M. N. H.; Manir, M. S.; Karim, M. R.; Khan, M. A. Efficiency Enhancement of Natural Dye Sensitized Solar Cell by Optimizing Electrode Fabrication Parameters. Mater. Sci. 2017, 35, 816– 823, DOI: 10.1515/msp-2017-008611

[62]. Hossain, M. K.; Rahman, M. T.; Basher, M. K.; Afzal, M. J.; Bashar, M. S. Impact of Ionizing Radiation Doses on Nanocrystalline TiO_2 Layer in DSSC's Photoanode Film. Results Phys. 2018, 11, 1172– 1181, DOI: 10.1016/j.rinp.2018.10.006

[63]. Son, DY., Lee, JW., Choi, Y. et al. Self-formed grain boundary healing layer for highly efficient $CH_3NH_3PbI_3$ perovskite solar cells. Nat Energy **1**, 16081 (2016). DOI:10.1038/nenergy.2016.81

[64]. D. Wei et al., "A TiO2 embedded structure for perovskite solar cells with anomalous grain growth and effective electron extraction,"J.Mater.Chem. A, vol. 5, no. 4, pp. 1406–1414, Dec. 2016, DOI: 10.1039/C6TA10418E.

[65]. Nabarun Saha, Giuseppe Brunetti , Mario N. Armenise and Caterina Ciminelli., "A strategy to simplify the preparation process of perovskite solar cells by co-deposition of a hole-conductor and a perovskite layer," Adv. Mater., vol. 28, no. 43, pp. 9648–9654, Sep. 2016, DOI: 10.1002/adma.201603850.

[66]. Yongzhen Wu, Xudong Yang, Wei Chen, Youfeng Yue, Molang Cai, Fengxian Xie, Enbing Bi, Ashraful Islam & Liyuan Han, "Perovskite solar cells with 18.21% efficiency and area over 1 cm^2 fabricated by heterojunction engineering," Nature Energy, no. 1, no. 11, pp. 1–7, Sep. 2016, DOI: 10.1038/nenergy.2016.148.

[67]. Chen, K., Wang, Q., Niu, Z. & Chen, J. Graphene-based materials for flexible energy storage devices. J. Energy Chem. 27(1), 12–24 (2018). DOI:10.1016/J.JECHEM.2017.08.015

[68]. Wang, M., Duan, X., Xu, Y. & Duan, X. Functional three-dimensional graphene/polymer composites. ACS Nano 10(8), 7231–7247 (2016). DOI:10.1021/acsnano.6b03349

[69]. Sun, P., Wang, K. & Zhu, H. Recent developments in graphene-based membranes: Structure, mass-transport mechanism and potential applications. Adv. Mater. 28(12), 2287–2310 (2016). DOI: 10.1002/adma.201502595

[70]. Huang, H., Chen, W., Chen, S. & Wee, A. T. S. Bottom-up growth of epitaxial graphene on 6H-SiC(0001). ACS Nano 2(12), 2513–2518 (2008). DOI: 10.1021/nn800711v

[71]. Hirata, M., Gotou, T., Horiuchi, S., Fujiwara, M. & Ohba, M. Thin-film particles of graphite oxide 1: High-yield synthesis and flexibility of the particles. Carbon 42(14), 2929–2937 (2004). DOI: 10.1016/j.carbon.2004.07.003

[72]. Stankovich, S. et al. Stable aqueous dispersions of graphitic nanoplatelets via the reduction of exfoliated graphite oxide in the presence of poly(sodium 4-styrenesulfonate). J. Mater. Chem. 16(2), 155–158 (2006). DOI: 10.1039/B512799H

[73]. A. Hosen, M.S. Mian, S.R. Al Ahmed, Improving the performance of lead-free $FASnI_3$ -based perovskite solar cell with Nb 2 O 5 as an electron transport layer, Adv. Theory Simulations 6 (2023) 2200652, DOI:10.1002/adts.202200652.

[74]. T. Zhang, H. Li, H. Ban, Q. Sun, Y. Shen, M. Wang, Efficient CsSnI 3 -based inorganic perovskite solar cells based on a mesoscopic metal oxide framework via incorporating a donor element, J. Mater. Chem. A. 8 (2020) 4118–4124, DOI:10.1039/C9TA11794F.

[75]. T. Ye, K.K. Wang, Y. Hou, D. Yang, N. Smith, B. Magill, J. Yoon, R.R.H.H. Mudiyanselage, G.A. Khodaparast, K.K. Wang, S. Priya, Ambient-air-stable lead-free CsSnI 3 solar cells with greater than 7.5% efficiency, J. Am. Chem. Soc. 143 (2021) 4319–4328, DOI:10.1021/jacs.0c13069.

[76]. X. Xu, J. Wang, D. Cao, Y. Zhou, Z. Jiao, Design of all-inorganic hole-transport-material-free $CsPbI_3$/$CsSnI_3$ heterojunction solar cells by device simulation, Mater. Res. Express 9 (2022) 025509, DOI:10.1088/2053-1591/ac5778.

PAPER NAME

Shreya Plag check document for report.pdf

AUTHOR

Shreya

WORD COUNT

8395 Words

CHARACTER COUNT

44348 Characters

PAGE COUNT

34 Pages

FILE SIZE

1.4MB

SUBMISSION DATE

Jun 3, 2024 1:29 PM GMT+5:30

REPORT DATE

Jun 3, 2024 1:30 PM GMT+5:30

4% Overall Similarity

The combined total of all matches, including overlapping sources, for each database.

- 3% Internet database
- 2% Publications database
- Crossref database
- Crossref Posted Content database
- 2% Submitted Works database

Excluded from Similarity Report

- Bibliographic material
- Quoted material
- Cited material
- Small Matches (Less then 10 words)

Gmail **Shreya Vasu <shreyavasu219@gmail.com>**

Fwd: Decision Letter (RAFM_09)

Shreya Vasu <shreyavasu219@gmail.com> Thu, Jun 6, 2024 at 4:35 PM
To: Shreya Vasu <shreyavasu219@gmail.com>

---------- Forwarded message ---------
From: **Suresh Sharma** <suresh321sharma@gmail.com>
Date: Thu, Jun 6, 2024 at 4:01 PM
Subject: Fwd: Decision Letter (RAFM_09)
To: Shreya Vasu <shreyavasu219@gmail.com>, Shikha Singh <shikhasingh10322@gmail.com>

Prof. Suresh C. Sharma
Former Dean (Academic-PG)
Former Head, Department of Applied Physics,
Delhi Technological University (DTU),
Govt. of NCT of Delhi,
Shahbad Daulatpur, Bawana Road, Delhi-110042, India
Email:suresh321sharma@gmail.com, prof_sureshsharma@dtu.ac.in

Former Chairman, Department Research Committee(DRC)[Applied Physics] DTU, Delhi.
Former Chairman, Board of Studies (BOS)[Applied Physics] DTU, Delhi
Young Scientist Project Awardee (DST, Govt. of India).
Monbusho Post-doctoral Fellowship Awardee (Govt. of Japan).
JSPS (Invitation) Post-doctoral Fellowship Awardee (Govt. of Japan).
Senior Research Associate under the Scientist's Pool Scheme Awardee (CSIR, Govt. of India).
Commendable Research Award for Excellence in Research Awarded by DTU, Delhi for six consecutive years i.e., March 21, 2018, March 19, 2019 , March 13, 2020, February 15, 2021, March 3, 2022 & April 6, 2023.

---------- Forwarded message ---------
From: **RAFM-2024, Department of Physics ARSD College** <rafm@arsd.du.ac.in>
Date: Thu, Jun 6, 2024 at 4:48 PM
Subject: Decision Letter (RAFM_09)
To: Suresh Sharma <suresh321sharma@gmail.com>

Ms. Ref. No.: RAFM_09
Title: Analytical Modelling and Numerical Simulation of Plasma Assisted Graphene Based Solar Cells

Dear Prof. Suresh C. Sharma,

I am pleased to inform you that your paper "An Analytical Modelling and Numerical Simulation of Plasma Assisted Graphene Based Solar Cells" has been accepted for publication in **"Select Springer Nature Proceedings of RAFM 2024 (Scopus Indexed)".**

Regards

Editor, RAFM-2024

PROOF OF SCOPUS INDEXING

PUBLICATION

Research papers presented in the conference and accepted after review through due process will be published in the Scopus indexed and peer-reviewed journals.

Springer

- Springer Nature (SCOPUS)
- IONICS, Springer (SCOPUS)

- Current Natural Science & Engineering, VVBF

About Scopus

Select papers from the conference will be published by Springer as a proceedings book volume. Springer will conduct quality checks on the accepted papers, and only papers that pass these checks will be published.

Disclaimer:

Springer Nature does not charge any money for the publication of Non-Open Access content. Abstracts/extended abstracts and short papers (less than 4 pages) are not considered for publication.

ATMA RAM SANATAN DHARMA COLLEGE

UNIVERSITY OF DELHI

Accredited Grade 'A++' By NAAC || All India 6th Rank in NIRF (Ministry of Education)

2nd International Conference on

Recent Advances in Functional Materials (RAFM-2024)

Under the aegis of IQAC and DBT (GoI) star college scheme

Certificate of Oral Presentation

This is to certify that Prof./Dr./Mr./Ms.

SHREYA VASU

Delhi Technological University, New Delhi

has presented his/her research work as oral presentation titled

Analytical Modeling and Numerical Simulation of Plasma Assisted Graphene Solar Cells

in 2nd International Conference on "Recent Advances in Functional Materials" (RAFM-2024) organised by Department of Physics under the aegis of IQAC ARSD College, University of Delhi & DBT (GoI) Star College during March 14-16, 2024 via online mode.

Dr. Manish Kumar
Convener, RAFM-2024

Prof. Vinita Tuli
Coordinator, IQAC

Prof. Gyantosh Kumar Jha
Principal, ARSD College

Certificate No: **ARSD/RAFM-2024/OT/161**

ATMA RAM SANATAN DHARMA COLLEGE

UNIVERSITY OF DELHI

Accredited Grade 'A++' By NAAC || All India 6th Rank in NIRF (Ministry of Education)

2nd International Conference on

Recent Advances in Functional Materials (RAFM-2024)

Under the aegis of IQAC and DBT (GoI) star college scheme

Certificate of Oral Presentation

This is to certify that Prof./Dr./Mr./Ms.

SHIKHA SINGH

Delhi Technological University, New Delhi

has presented his/her research work as oral presentation titled

Analytical Modeling and Numerical Simulation of Plasma Assisted Graphene Solar Cells

in 2nd International Conference on "Recent Advances in Functional Materials" (RAFM-2024) organised by Department of Physics under the aegis of IQAC ARSD College, University of Delhi & DBT (GoI) Star College during March 14-16, 2024 via online mode.

Dr. Manish Kumar
Convener, RAFM-2024

Prof. Vinita Tuli
Coordinator, IQAC

Prof. Gyantosh Kumar Jha
Principal, ARSD College

Certificate No: **ARSD/RAFM-2024/OT/160**

Gmail **Shreya Vasu <shreyavasu219@gmail.com>**

Fwd: Acceptance Letter for 2nd International Conference on Recent Advances in Functional Materials (RAFM-2024)

Shreya Vasu <shreyavasu_2k22mscphy51@dtu.ac.in> Thu, Jun 6, 2024 at 9:46 AM
To: Shreya Vasu <shreyavasu219@gmail.com>

---------- Forwarded message ---------
From: <rafm@arsd.du.ac.in>
Date: Mon, Feb 19, 2024 at 7:21 PM
Subject: Acceptance Letter for 2nd International Conference on Recent Advances in Functional Materials (RAFM-2024)
To: <shreyavasu_2k22mscphy51@dtu.ac.in>

ACCEPTANCE LETTER

Dear **Ms. Shreya Vasu**
DELHI TECHNOLOGICAL UNIVERSITY
Greetings!!

ARSD College welcomes you to the 2nd International conference on Recent Advances in Functional Materials (RAFM-2024).

RAFM-2024 to be held online mode at Atma Ram Santan Dharma College, University of Delhi during March 14-16, 2024, which is being organized by Department of Physics, IQAC and STAR College Scheme (GOI). Its matter of great pleasure that the technical committee accepted your research paper entitled:

ANALYTICAL MODELING AND NUMERICAL SIMULATION OF PLASMA ASSISTED GRAPHENE SOLAR CELLS

You are invited for a presentation of the same at RAFM-2024 as **Oral Presentation.**

Time allotted for oral presentation is **10 (8+2) Min.** and the participant is requested to report and present online your paper within stipulated time.

Thank You

--

Dr. Manish Kumar

(Convener, RAFM-2022)

Assistant Professor

Department of Physics, ARSD College

University of Delhi, Dhaula Kuan, New Delhi-110021

Email: mkumar2@arsd.du.ac.in

Mob.: +919555977892